

Controlled Molecular Magnetism of Bi- and Polynuclear Transition Metal Complexes Based on Hydrazones, Azomethines, and Their Analogs

V. V. Lukov^a, *, I. N. Shcherbakov^a, S. I. Levchenkov^{a, b}, Yu. P. Tupolova^a, L. D. Popov^a,
I. V. Pankov^a, and S. V. Posokhova^c

^aSouthern Federal University, Rostov-on-Don, Russia

^bSouthern Scientific Center, Russian Academy of Sciences, Rostov-on-Don, Russia

^cAzov Black Sea Engineering Institute, Don State Agrarian University, Zernograd, Russia

*e-mail: vlukov@mail.ru

Received April 13, 2018; revised July 12, 2018; accepted September 5, 2018

Abstract—The possibilities of the magnetochemical method for the description of structures and properties of bi- and tetranuclear metallochelates and supramolecular architectures based on coordination compounds with restricted types of ligand systems, mainly hydrazones, azomethines, and their analogs, are reviewed. The known published data for the bi- and polynuclear complexes, whose paramagnetic centers are bound by both intra- and intermolecular exchange interactions, are systematized. A relationship between specific features of the electronic and geometric structures of the complexes and the character of the exchange effects is considered. Magnetostructural relations in the discussed compounds are systematized. The compounds discussed are important model objects for the development of the strategy for the targeted design of one-, two-, and three-dimensional magnetically ordered structures.

Keywords: magnetochemistry, exchange-bound complexes, quantum chemical calculations, exchange parameters, magnetostructural relations, hydrazones, azomethines, molecular magnetics

DOI: 10.1134/S1070328419030060

INTRODUCTION

The synthesis and analysis of the physicochemical properties of the polynuclear metal complexes with magnetic and electronic interactions between the metal centers are among the central trends of the studies of the modern coordination chemistry, molecular electronics, and molecular biology [1–17]. It is evident from the fundamental point of view that the exchange interaction and electron transfer are tightly interrelated processes based on the effects of the interaction between the spin and electrostatic charge of electrons. Electron transport in electronic devices or metalloproteins is a remarkable example for the inter-electron interaction in artificial and natural systems, respectively. It should be mentioned that molecular magnetics (single-molecule magnets, SMM) and polynuclear coordination compounds exhibiting the spin-crossover effect can be considered as very convenient systems modeling unique magnetic properties characteristic of usual inorganic magnetic materials (metallic alloys and metal oxides) and supplementing them by technologically significant optical, electronic, chemosensor, and adsorption properties [18–22]. It seems doubtless that detailed experimental and

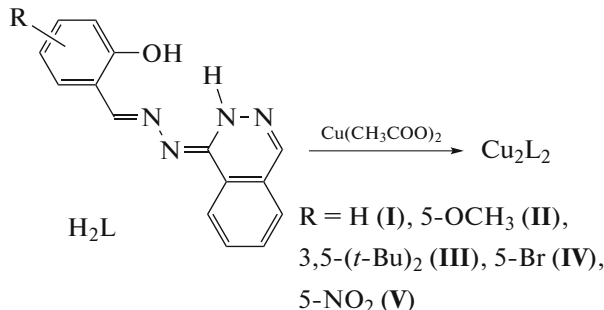
theoretical analyses of similar systems would allow researchers of molecular magnetism to discover basically new classes of externally controlled multifunctional molecular magnetic materials [23]. On the one hand, porous and luminescent magnets, objects of nonlinear optics, multiferroics, and proton and electron magnetic conductors and, on the other hand, thermo-, piezo-, photo-, or chemoswitchable magnets are bright illustrative examples for nanotechnological systems of the nearest future [24–35]. It is commonly accepted that the classical works by R. Hoffmann and O. Kahn [36–41] served as a theoretical basis for the vigorous development of the main statements of molecular magnetism. Further the works of these scientists and their research groups developed the ways of the rational design and synthesis of exchange-bound homo- and heterobinuclear transition metal complexes with predicted magnetic properties and thus illustrated the ability of researchers to convert natural materials according to the tasks of scientific and technical progress [42–45]. Nevertheless, the investigation of the electronic structures and properties of the polynuclear complexes containing two or more paramagnetic centers bound by the exchange interaction at the moment remains to be one of the

most urgent problems of coordination chemistry [17, 46, 47]. The elucidation of a relationship of the exchange interaction parameters with specific structural features of polynuclear complexes plays the key role in the understanding of the magnetic properties of similar systems and forms a theoretical basis for the synthesis of exchange-bound systems with specified magnetic characteristics and finally for the targeted modification of magnetically active materials [48–50]. In the present review, we attempted to systematize the known literature data for the bi- and polynuclear complexes, whose paramagnetic centers are bound by both intra- and intermolecular exchange interactions with the ligands based on the organic derivatives of hydrazine and Schiff bases and related systems. Evidently, potent magnetostructural relationships obtained for these classes of compounds can be very useful for the solution of a broader range of problems indicated above. The specific features of the structures and magnetic properties of the tetranuclear complexes, whose oligomeric structure is an important intermediate unit between the “classical” binuclear derivatives and polymeric supramolecular architectures, are considered in a special chapter.

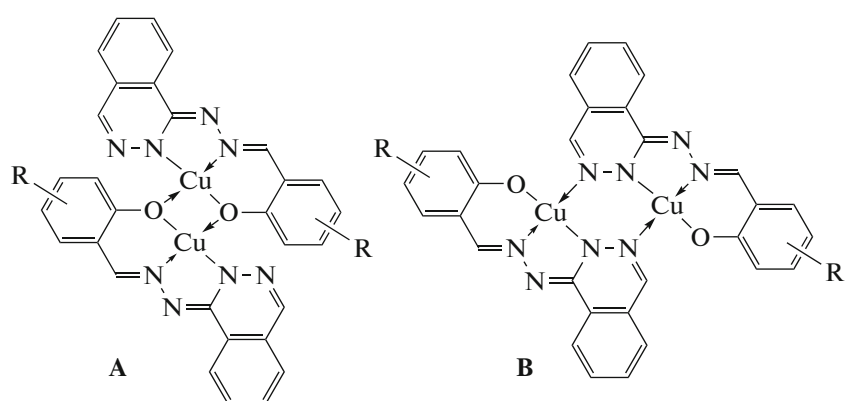
I. MAGNETOSTRUCTURAL RELATIONSHIPS IN THE BINUCLEAR COMPLEXES CONTAINING HETERO CYCLIC FRAGMENTS

Hetarylhydrazones of carbonyl compounds are popular objects of the modern organic and coordination chemistry due to their biological activity. There are numerous published data on their antibacterial, antiviral, antitumor, and antispasmodic activity [51–58]. Many hetarylhydrazones are chromogenic agents, extracting agents, and analytical sensors to metal ions [59, 60]. The high complexation activity of hetarylhydrazones combined with the relative easiness of the synthetic variation of structural details in these systems makes it possible to obtain binuclear complexes being, as mentioned above, convenient models for studying the main factors determining the character and strength of exchange interactions between the paramagnetic centers due to the possibility of varying

the nature of the donor centers, central ions, and exogenic bridging groups. The exchange can be both antiferro- and ferromagnetic. For example, the results of the synthesis, physicochemical study, and quantum chemical modeling of the binuclear copper(II) complexes with 1'-phthalazinylhydrazones of substituted salicylaldehydes are presented [61].



The binuclear structures of compounds I–V were confirmed by the observation of a strong antiferromagnetic exchange interaction between the copper(II) ions, and the presence of the phthalazine fragment in hydrazones H_2L substantially extends potential possibilities of these ligand systems in the formation of binuclear complexes. The earlier described salicylaldehyde hetarylhydrazones can form dimeric complexes only if the phenoxide oxygen atoms perform the bridging function [62–64]. The structure of hydrazones H_2L predetermines two possible dimerization modes: through the phenoxide atoms of the aldehyde fragment to form the four-membered metallochelate cycle $\text{Cu}-\text{O}(\text{O}')-\text{Cu}$ or via the atoms of the phthalazine fragment to form the six-membered cycle $\text{Cu}-\text{N}-\text{N}'(\text{N}''-\text{N}''')-\text{Cu}$. In this respect, hydrazones H_2L are similar to salicylaldehyde acyl- and aroylhydrazones, which are also characterized by two dimerization modes: via the phenoxide or α -oxyazine oxygen atoms of the aldehyde or hydrazone fragments, respectively [65]. Thus, dimeric structures of the A or B types can be formed for binuclear complexes I–V.



In the case of complex **III**, the *tert*-butyl group in the *ortho*-position to the phenol group excludes the possibility for dimer structure **A** to take place [66]. The fact that complex **III** is undoubtedly binuclear because of a strong antiferromagnetic exchange ($2J = -416 \text{ cm}^{-1}$) unambiguously indicates that the **B** type structure occurs, in this case, with dimerization via the diazine bridges. In other cases, any isomeric structure can theoretically be formed.

A substantial distinction between the binuclear copper(II) complexes with 1'-phthalazinylhydrazones of the salicylaldehyde derivatives and the dimeric copper(II) complexes with acylhydrazones is the character of the magnetic exchange interaction in the coordination isomers. In the case of salicylaldehyde acylhydrazones, different dimerization modes lead to a substantial difference in the magnetic properties of the isomers [66–71]. In both cases, the exchange is antiferromagnetic, but a stronger exchange interaction is observed for dimerization via the phenoxide atoms in the complexes. In this case, the exchange parameters range from -300 to -500 cm^{-1} versus the range from -50 to -150 cm^{-1} for dimerization via the α -oxyazine oxygen atoms [8, 24]. This difference in the magnetic properties enables one to determine the structure of the isomer from the magnetochemical data. However, the so-called “magnetochemical criterion of isomer structure determination” [72] is inappropriate for the binuclear copper(II) complexes with 1'-phthalazinylhydrazones of the salicylaldehyde derivatives, because a strong antiferromagnetic exchange takes place in the complexes of various phthalazinylhydrazones via the diazine bridges [73–75].

We performed the quantum chemical calculation of the exchange parameters by the density functional theory (DFT) for the theoretical interpretation of the influence of the dimerization mode in binuclear complexes **I–V** on the exchange interaction. The molecular structures of dimers **A** and **B** ($R = H$) in *vacuo* according to the calculation data are shown in Fig. 1.

In all cases, the optimization of the geometry results in the structures with the nonplanar exchange fragment. The four-membered cycle $\text{Cu}–\text{O}(\text{O}')–\text{Cu}$ in dimers **A** is slightly distorted because of the inflection along the line connecting the bridging oxygen atoms, and the dihedral angle between the root-mean-square planes of the coordination polyhedra of the copper atoms is $\sim 30^\circ$ (Fig. 1). The copper–copper distances in dimers **A** are independent of the nature of substituent R and are equal to 2.97 – 2.98 \AA .

According to the data of X-ray diffraction analysis (XRD), the copper–copper distance in the copper(II) complexes with salicylaldehyde hydrazones in which dimerization occurs via the phenoxide oxygen atom is 3.01 – 3.05 \AA [76–80], which is very close to the calculation results for the geometry of dimers **A**. Some underestimation of the distance is caused by the aforementioned distortion of the exchange fragment, which

is usually quite planar according to the XRD data. According to the results of the geometry calculations, the six-membered exchange fragment $\text{Cu}–\text{N}(\text{N}'–\text{N}'')–\text{Cu}$ in dimers **B** has a boat conformation with the copper atoms in the apical positions (Fig. 1b). As in the previous case, the nature of substituent R weakly affects the degree of distortion of the exchange fragment, and the copper–copper distances are fairly close (3.70 – 3.73 \AA). A comparison of the total energies of the triplet states of dimers **A** and **B** shows that the dimerization via the nitrogen atoms of the phthalazine fragments is more favorable. The total energy of dimers **B** is by 8.8 – 12.9 kcal/mol lower than that of dimers **A**, which is fairly substantial. This suggests that dimerization in complexes **I–V** occurs via the phthalazine bridges. A good argument in favor of this assumption is the dimeric character of complex **III** for which, as said above, the dimerization via the phenoxide atoms (structure **A**) is excluded for steric reasons.

The calculated and experimental exchange parameters in dimeric structures **A** and **B** are presented in Table 1. For dimers **A** (with dimerization via the phenoxide oxygen atom), the absolute value of the exchange parameter for any substituent R is appreciably higher than that for dimers **B**. However, on the whole, the quantum chemical modeling results for the exchange interaction in dimers **A–B** do not allow one to unambiguously choose between the coordination isomers of complexes **I–V**, although the calculated values of $2J$ for dimers **B** with the dimerization via the phthalazine fragments are better consistent with the experiment.

Thus, only the experimental determination of the structures of the complexes can serve as a decisive argument in the problem of choosing between the coordination isomers of complexes **I–V**. Unfortunately, attempts to obtain single crystals of the binuclear complexes suitable for XRD failed and, hence, another experimental method capable of providing information on the structures of the complexes was used: X-ray absorption spectroscopy that makes it possible to determine the local structure of the coordination sphere of transition metal ions. The structural parameters of the coordination modes in complexes **I–V** obtained in the framework of this method are close, which proves that the same dimerization mode occurs in all compounds. The value of the copper–copper distance enables one to draw the experimentally substantiated conclusion about the dimer structure. As mentioned above, the copper–copper distance in the complexes with the dimerization via the phenoxide atom of the salicylaldehyde fragment cannot exceed 3.1 \AA . Since the determination inaccuracy of the metal–metal distance by the EXAFS method is about 0.02 – 0.05 \AA [81, 82], the data obtained make it possible to unambiguously exclude the formation of dimeric structures **A**. According to the EXAFS data, the shorter $\text{Cu}–\text{Cu}$ distance compared to the calculated one can be caused by the distortion of the struc-

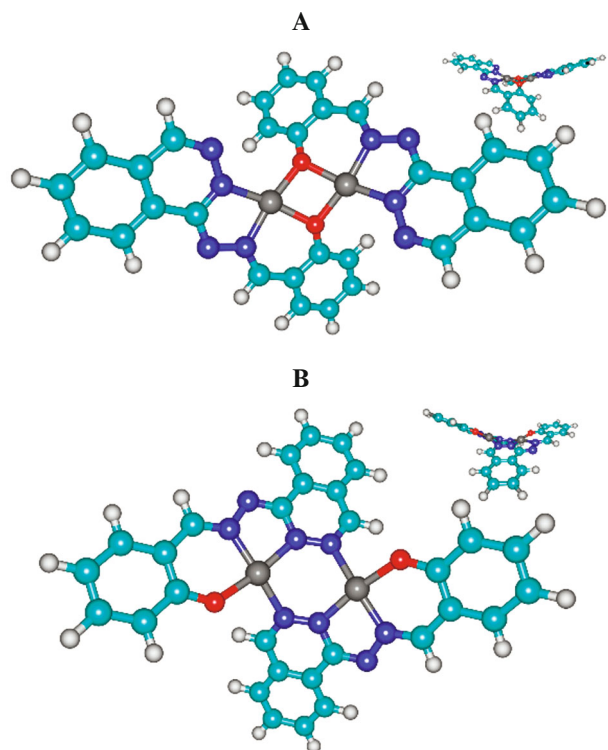
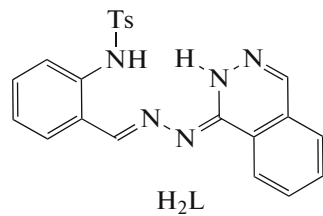


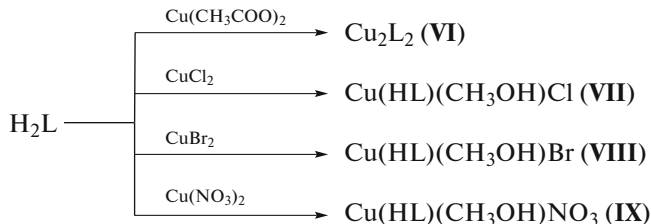
Fig. 1. Molecular structures of dimers **A** and **B** according to the calculation data, R = H (the view in another projection is shown at upper right) [61].

ture of the binuclear molecule due to intermolecular interactions in the crystal packing.

Thus, it can be asserted with high probability on the basis of the overall data of magnetochemistry, quantum chemical calculations, and X-ray absorption spectroscopy that the dimerization in the copper(II) complexes with 1'-phthalazinylhydrazones of the salicylaldehyde derivatives proceeds via the nitrogen atoms of the phthalazine fragments. It was unambiguously confirmed that the indirect exchange interaction between the copper(II) ions involving the phthalazine fragments has the pronounced antiferromagnetic character [83] by the physicochemical study of 2-(*N*-tosylamino)benzaldehyde 1'-phthalazinylhydrazone (H_2L) and the related transition metal complexes.



The complexes were synthesized according to the following scheme:



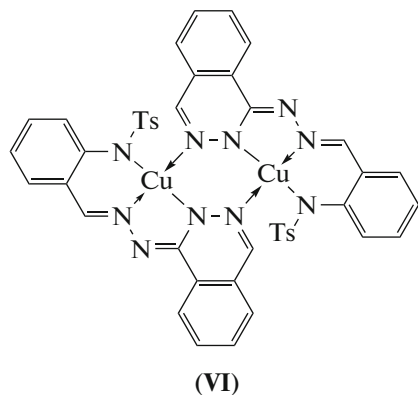
The Cu_2L_2 and $\text{Cu}(\text{HL})(\text{CH}_3\text{OH})\text{X}$ complexes (L^{2-} and HL^- are doubly and monodeprotonated forms of hydrazone; $\text{X} = \text{Cl}, \text{Br}$) (**VI**–**VIII**) were synthesized by the reactions of hydrazone H_2L with copper(II) acetate, chloride, and bromide. The reaction of hydrazone H_2L with copper(II) nitrate affords complex $\text{Cu}(\text{HL})(\text{CH}_3\text{OH})\text{NO}_3$ (type **IX**).

The measurement of the electric conductance of 0.001 M solutions of the complexes in DMF showed that complex **IX** can be assigned to binary electrolytes [84], indicating the out-of-sphere coordination of the nitrate anion in the composition of the complex. The data of IR spectroscopy indicate the coordination of the ligand with copper(II) acetate in the doubly deprotonated form and with copper(II) halides and nitrate in the monodeprotonated form. The effective magnetic moment (μ_{eff}) of complex **VI** at room temperature ($1.23 \mu_{\text{B}}$) is noticeably lower than the spin-only value ($1.73 \mu_{\text{B}}$) and decreases to $0.18 \mu_{\text{B}}$ on cooling to the boiling point of liquid nitrogen, and the exchange parameter $2J$ is -416 cm^{-1} . These data unambiguously show that the complex is dimeric. In this case, only one dimerization mode is possible for the complex: via the nitrogen atoms of the phthalazine fragment, because the bridging function of the nitrogen atom of the aldehyde fragment cannot almost be performed because of steric hindrances created by the tosyl group. The value of the exchange parameter in com-

Table 1. Calculated exchange parameters (cm^{-1}) in dimeric structures **A**–**B** and experimentally obtained values of $2J$ in complexes **I**–**V**

Compound	R	$2J_{\text{calcd}}$		$2J_{\text{exp}}$
		dimer A	dimer B	
I	H	−712	−595	−485
II	5-OCH ₃	−754	−593	−445
III	3,5-(<i>t</i> -Bu) ₂	—	−609	−416
IV	5-Br	−699	−606	−416
V	5-NO ₂	−642	−629	−402

plex **VI** is within the range characteristic of the binuclear copper(II) complexes with the diazine bridges ($2J$ from -300 to -600 cm^{-1} are presented for similar compounds) [85–87].

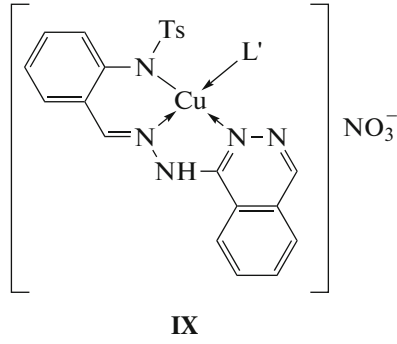
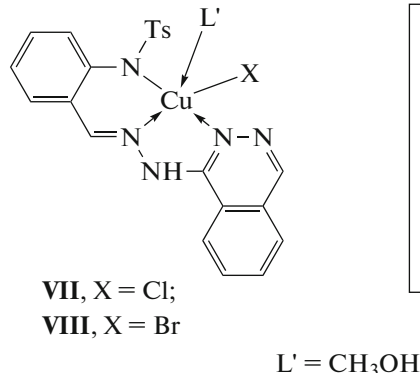


The structure of complex **VI** was also determined by XRD (Fig. 2), and the results of this method confirmed the conclusions made on the basis of the spectral and magnetochemical studies. The copper(II) ion in the molecule of the binuclear complex is pentacoordinated. Three sites in the coordination sphere of the Cu^{2+} ion are occupied by the nitrogen atoms of one ligand arranged at approximately the same distance from the copper ion: $\text{Cu}(1)-\text{N}(1)$ 1.934(7), $\text{Cu}(1)-\text{N}(2)$ 1.944(8), and $\text{Cu}(1)-\text{N}(5)$ 1.937(8) \AA . The fourth site is occupied by the $\text{N}(4^{\#})$ atom of the second ligand at an appreciably longer distance ($\text{Cu}(1)-\text{N}(4^{\#})$ 2.014(8) \AA), and the dimerization of the mononuclear fragments occurs via this site to form the six-membered exchange cycle $\text{Cu}(1)-\text{N}(5)-\text{N}(4)-\text{Cu}(1^{\#})-\text{N}(5^{\#})-\text{N}(4^{\#})$. The coordination sphere of the copper ion is completed by the $\text{O}(2)$ oxygen atom of the tosyl fragment. The five-membered chelate cycle has an envelope conformation, whose “flap” is occupied by the copper atom deviated from the mean

plane of other four atoms by 0.171(1) \AA . The six-unit chelate cycle is distorted much more strongly because of the inflection along the $\text{N}(1)-\text{C}(7)$ and $\text{N}(1)-\text{N}(2)$ lines. The structures of the monomeric complex fragments are close to planar (except for the tosyl fragments being in the “flagstaff” conformation relative to the ligand plane). The planes of two monomeric fragments form a dihedral angle of 64.4°. As a result, unlike the earlier described complexes with the phthalazine bridging groups [85], the plane of the six-membered exchange fragment in complex **VI** is considerably distorted and its conformation is close to the boat conformation with the copper atoms in the apical positions. The copper atoms are arranged at a distance of 3.367(1) \AA from each other. For the described [88] binuclear copper(II) complex with 2-acetylbenzimidazole 1'-phthalazinylhydrazone in which steric hindrances are less substantial, the quantum chemical calculation gives a similar structure of the exchange fragment. Owing to the steric repulsion, the planes of the phenyl rings of the tosyl fragments in the structure of complex **VI** are nearly planar and the angle between them is ~9°.

The quantum chemical modeling of the exchange interaction in complex **VI** was performed in terms of the broken symmetry technique. The antiferromagnetic exchange parameter $2J = -457$ cm^{-1} calculated in this approximation agrees satisfactorily with the value determined from the experimental data ($2J = -416$ cm^{-1}).

The effective magnetic moments of complexes **VII–IX** are close to the spin-only values for the Cu^{2+} ion and remain almost unchanged on cooling. No exchange interaction between the Cu^{2+} ions and other results of the physicochemical study allowed the authors to ascribe with high probability the following monomeric structures to these complexes:



At the same time, only magnetochemical data enable fairly reliable structure assignment for some exchange-bound complexes with phthalazinylhydrazones. This is

indicated by the results [89] of the physicochemical study of hetarylhydrazones of glyoxalic acid **X** and the related transition metal complexes.

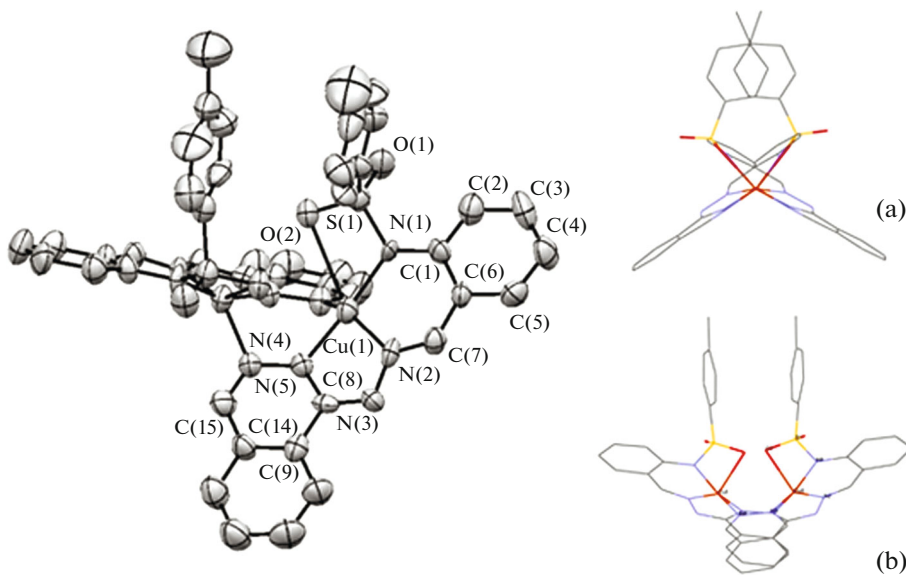
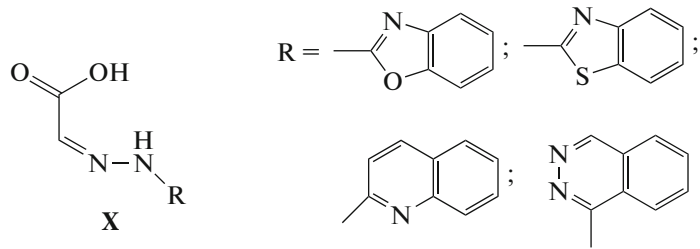
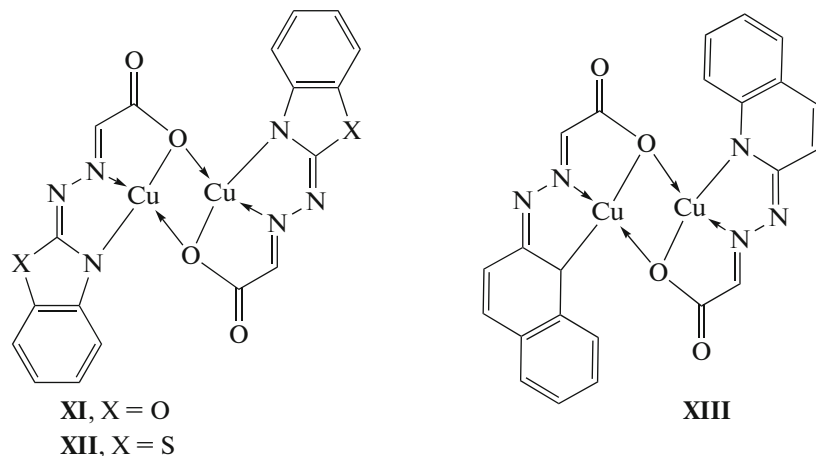


Fig. 2. Structure of complex VI (hydrogen atoms are omitted, and thermal vibration ellipsoids are presented with 50% probability) and the projections of the structure of the complex (a) along the Cu–Cu line and (b) perpendicularly to the Cu–Cu line [83].



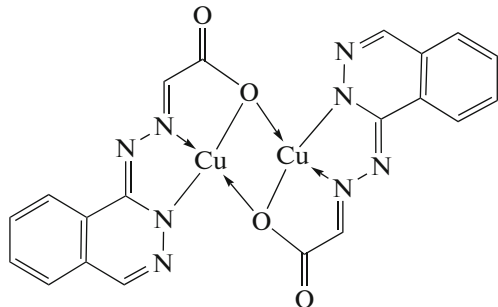
According to the data of XRD and electronic, IR, and NMR spectroscopy, the known hydrazones based on 1-hydrazinophthalazine exist in the free state as phthalazone tautomers (mixed azines) [90]. Metallochelates Cu_2L_2 , where L is the doubly deprotonated form of hydrazones, were obtained by the reactions of hydrazones X with copper(II) acetate. The measurement of the magnetic susceptibility of the complexes

shows that for all compounds the values of μ_{eff} per one copper ion at room temperature are substantially lower than the spin-only value and decrease on cooling to the boiling point of liquid nitrogen, indicating the exchange interaction of the antiferromagnetic type between two copper ions and suggesting the dimeric structure of the XI–XIII type metallochelates.

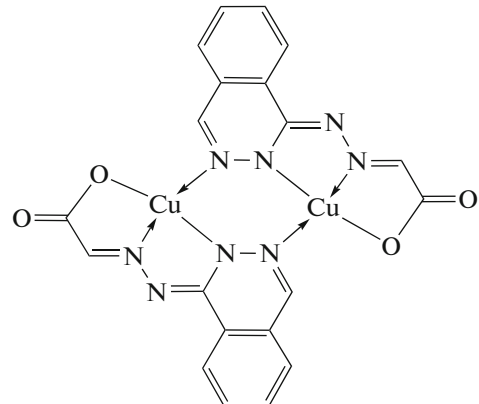


The dimerization mode of the complexes based on these hydrazones is unambiguously specified by the ligand structure, since the bridging function cannot be performed by the heterocyclic nitrogen atoms in this case. In the case of the complex based on phthalazinylhydrazone of the **X** type, the

dimerization of the mononuclear fragments of the complex can proceed via both the oxygen atoms of the carboxyl group and the diazine chain of the nitrogen atoms of the phthalazine fragment with the formation of structures of the **XIV** and **XV** types, respectively.



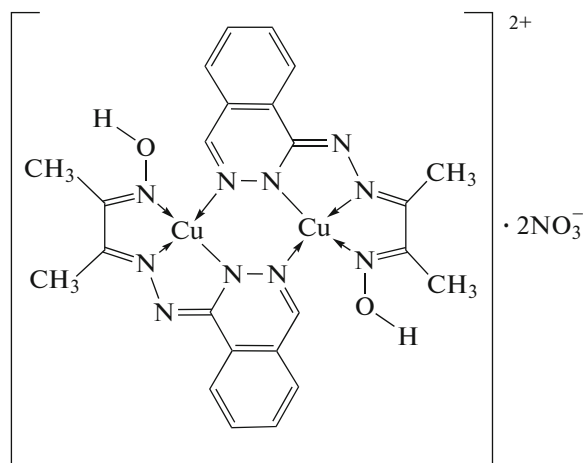
(XIV)



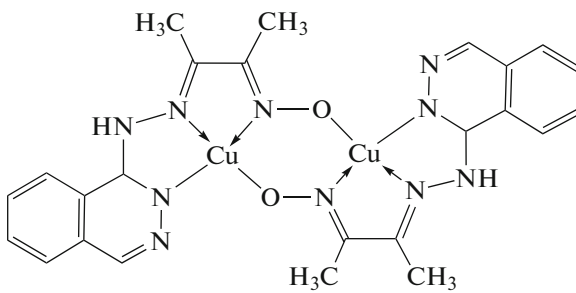
(XV)

As shown by the magnetochemical analysis results, this complex, as complexes **XI–XIII**, is characterized by the insignificant antiferromagnetic exchange interaction ($2J = -136 \text{ cm}^{-1}$). According to the developed [65, 72] concept of geometric modeling of the exchange fragments of the binuclear transition metal complexes with hydrazones, this value of the exchange parameter indicates the formation of the dimeric structure of the **XIV** type. In the case of the **XV** type binuclear structure, the exchange interaction parameter should be substantially higher by absolute value [91–93].

A combination of the magnetochemical experiment, quantum chemical calculations, and EXAFS data makes it possible to almost unambiguously conclude in favor of the formation of a certain structure of the exchange-bound complexes with the phthalazinylhydrazone ligands even without XRD data, which is indicated by published results [94]. The results of studying the structures of the diacetylmonooxime 1'-phthalazinylhydrazone complexes obtained by the reactions with copper(II) nitrate (complexes **XVI–XVIa**) are presented in this work.



(XVI)



(XVIa)

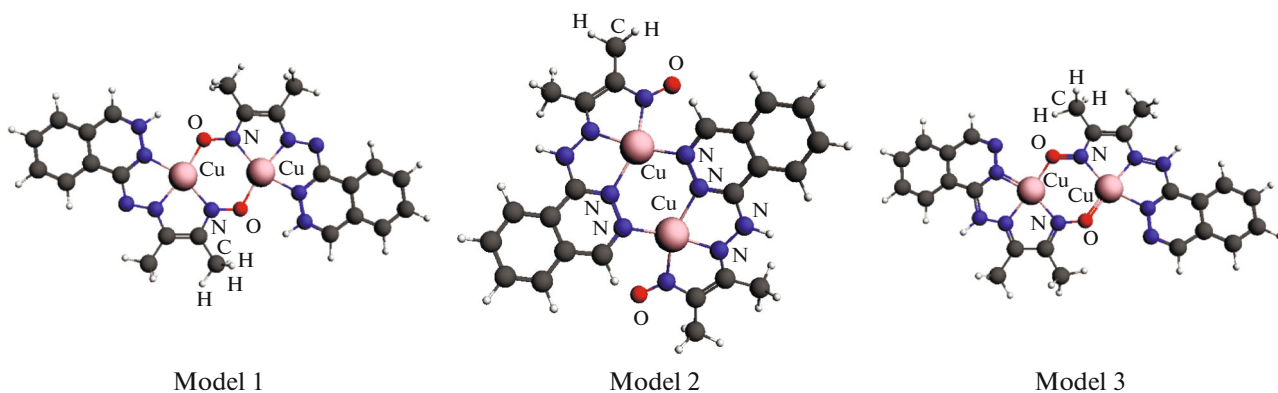


Fig. 3. Isomeric geometric models of complex XVI [94].

The structural models of complexes XVI–XVIa were proposed on the basis of geometric modeling using the standard bond lengths and bond angles. The spatial structures of the models of the XVI type complex are shown in Fig. 3.

The optimized structural models of complex XVI were further used for the calculation of X-ray absorption spectra (XANES). It turned out that the spectrum calculated for structural model 2 gave the best agreement with the experimental XANES spectrum. To refine the most probable models of the structure of complex XVI, this study was supplemented by the counter quantum chemical modeling of the exchange interaction. The antiferromagnetic exchange interaction in this complex is fairly high ($2J = -295 \text{ cm}^{-1}$). The exchange value and data of the physicochemical study indicate that in this compound the bridging function can be performed by either the nitrogen atoms of the phthalazine fragments (the complex has the structure of XVI) or the atoms of the nitroso groups, which corresponds to structure XVIa. In both cases, the exchange fragment should be close to planar, which would favor the efficient overlapping of the “magnetic” atomic $d_{x^2-y^2}$ orbitals of the copper(II) ions involving the orbitals of the bridging atoms.

We calculated $2J$ for alternative structures of the complexes (Table 2) in terms of the broken symmetry approach to estimate the magnetic exchange parameter for possible isomers and to compare them with the experimentally measured values.

In the case of the XVI type dicationic complexes formed due to the out-of-sphere coordination of the nitrate anions, the interaction is antiferromagnetic for all considered isomeric structures, and only the value of the interaction differ sharply (Table 2). The coordination mode via the nitroso group ($\text{N}=\text{O}$ chain) determines a very strong interaction: $2J = -1640$ or -1536 cm^{-1} for models 1 and 3, respectively. In the case of model 2 (dimerization via the diazine chains of the phthalazine fragments), the singlet–triplet splitting is 379 cm^{-1} , which corresponds to the experimentally

obtained value ($2J = -295 \text{ cm}^{-1}$) and agrees with the above presented XANES results.

It can be stated that heterocyclic, primarily phthalazinyl, bridges are very convenient objects for experimental and theoretical analyses of specific features of the manifestation of exchange effects in the binuclear metallochelates based on the hydrazone ligands. Similar systems can also be used as convenient linkers and for the preparation of chain polymeric exchange-bound structures [95–100]. The authors of these studies mention that such electronic and geometric factors as bridge compositions, bond and dihedral angles in the exchange-bound chelate cycles, and the internuclear distance between the paramagnetic centers are the main factors in the formation of an exchange interaction of certain nature and strength. These systems are important model objects in the development of the strategy of targeted design of one-, two-, and three-dimensional magnetically ordered structures that open a new chapter in the physical chemistry of controlled molecular magnetism. In many cases, this ordering occurs due to effects of the intermolecular magnetic interaction, and some important details of which are considered in the next section.

II. COMPLEXES WITH THE INTERMOLECULAR EXCHANGE INTERACTION TRANSLATED ALONG THE SYSTEM OF HYDROGEN BONDS

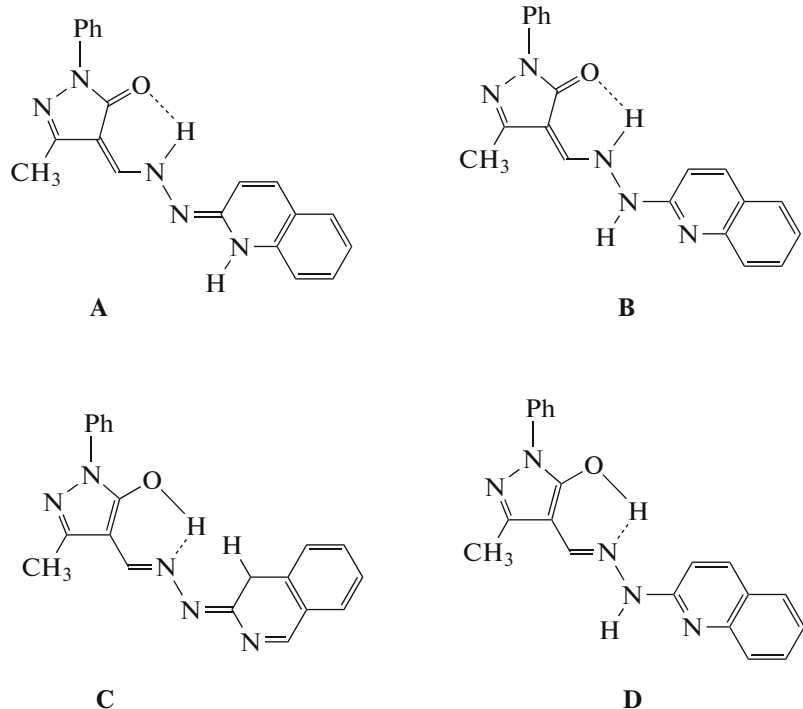
Intermolecular noncovalent interactions determining the molecular packing of functional nanosized materials can be considered as the major “driving force” or a means of controlling the magnetic exchange interaction in supramolecular architecture [101]. In particular, hydrogen bonds and cation-anionic, $\pi-\pi$, and van der Waals interactions between individual molecules can be used purposefully for the formation of exchange interaction channels the value of which can be predetermined by both the sign and absolute value [102]. As mentioned in the works cited above, in several cases, these interactions can be the

same or even more efficient in the formation of ferro-, antiferro-, and ferrimagnetics as the traditional covalent interactions determining the intramolecular character of the exchange.

At the same time, the targeted design of magnetic materials using noncovalent interactions is rather restricted, because similar effects, on the one hand, can act as organizers of the crystalline architecture and, in some cases, as mediators of the magnetic exchange between the metal centers. On the other hand, the character and manifestation of magnetic parameters is not such unambiguously predictable as in the case of the intramolecular exchange [103–108]. Therefore, the development of relatively new approaches to the theoretical modeling of the exchange in these objects taking into account diversity

of structural factors involved in intermolecular interactions, the nature of acceptor and donor atoms, the electronic nature of interacting metal centers, and others is urgent and important. The validity of the last statement is confirmed by the examples presented above.

The study [109] is devoted to the examination of the structure, magnetic properties, and quantum chemical modeling of the copper(II) complex of the **XVII** type with 1-phenyl-3-methyl-4-pyrazole-5-quinolylhydrazone in which the intermolecular exchange was detected in the channel of the NH···O hydrogen bond. Structure **A** was chosen of four possible tautomeric forms **A–D** as the most stable one for the indicated ligand system using NMR spectroscopy and quantum chemical calculations.



A similar structure of the ligand assumed the formation of the mononuclear copper(II) metallochelate, but the data of EPR spectroscopy and magnetochemical measurements showed a weak exchange interaction of the antiferromagnetic type between the copper ions. The signal with $g = 4.121$ corresponding to the forbidi-

den transition in the dimeric copper(II) complexes was detected in the EPR spectrum [110], which is confirmed by the magnetic properties of this compound. The magnetic properties were interpreted using Eq. (1) and taking into account both the pair and intermolecular exchanges

Table 2. Total energies (au) of the high-spin $E(\text{HS})$ and broken symmetry $E(\text{BS})$ states and the calculated values of $2J(\text{cm}^{-1})$ for the **XVI** type complexes

Type	$E(\text{HS})$	$E(\text{BS})$	$2J_{\text{calcd}}, \text{cm}^{-1}$
Model 1	–4908.232104	–4908.239578	–1640
Model 2	–4908.222266	–4908.223993	–379
Model 3	–4908.220893	–4908.227890	–1536

$$\chi_m = \frac{\chi_m'}{1 - 7.6853zJ'x_m'/g^2} \quad (1)$$

with the best approximation parameters $2J = -3.54 \text{ cm}^{-1}$ and $zJ' = -0.08 \text{ cm}^{-1}$. As expected, the molecule of complex **XVII** is mononuclear (Fig. 4).

In this connection, the exchange interaction can be explained by intermolecular association (Fig. 5).

Using the quantum chemical modeling of the exchange interaction, the authors of the cited work showed the formation of the structure presented in Fig. 6 with the exchange channel unusually extended along the chain of atoms Cu—N—N···H—O—C—O—Cu of two possible association modes (Figs. 6 and 7, respectively).

The phthalazinylhydrazone derivatives being, as shown in the previous section, convenient ligand systems for the formation of the exchange-bound complexes with the predictable and controlled character of exchange can also be used for the preparation of supramolecular architectures, primarily due to the additional donor centers and NH groups in the complexes [111–114]. The copper(II) complexes $[\text{CuL}^1(\text{NO}_3)_2]\text{CH}_3\text{OH}$ (**XVIII**) and $[\text{CuL}^2\text{Cl}]\text{CH}_3\text{OH}$ (**XIX**) (L^1 and L^2 are monodeprotonated residues of 3,5-di-*tert*-butylsalicylaldehyde 1'-phthalazinylhydrazone and 2-*N*-tosylaminobenzaldehyde 2-imidazolinylhydrazone, respectively) were synthesized [114]. The structures of complexes **XVIII** and **XIX** are shown in Fig. 8.

The methanol molecule in the crystal structure of complex **XVIII** forms two hydrogen bonds O(1S)—H(1)···O(2) and N(3)—H(3B)···O(1S), resulting in the formation of hydrogen-bound dimers packed in infinite piles extended along the crystallographic axis a (Fig. 9a).

In the case of complex **XIX**, each methanol molecule forms two hydrogen bonds with two nearest molecules of the complex. The NH groups of the imidazoline fragments and O(1S) atoms of the tosyl groups in these molecules also form two hydrogen bonds resulting in the formation in the crystal of complex **XIX** of hydrogen-bound dimers packed in infinite piles extended along the crystallographic axis c (Fig. 9b).

The structures of complexes **XVIII** and **XIX** assume the possibility of a magnetic exchange interaction between the copper(II) ions. In both cases, the possible exchange channel is fairly extended, and the N—H···O hydrogen bond should participate in the exchange translation [109]. The dimer of complex **XVIII** contains only one pair exchange channel in which the copper ions are separated by the linker containing six atoms and two hydrogen bonds: Cu—N—N···H—O—Cu, and the copper—copper distance is 5.208 Å. The dimer of complex **XIX** contains two alternative pair exchange channels: the chains of seven atoms with one hydrogen bond Cu—N=C—N—H···O=S—N—Cu and the chains of eight atoms with

two hydrogen bonds Cu—N—N—H···O—H···O=S—N—Cu, and the copper—copper distance is 5.756 Å.

Complexes **XVIII** and **XIX** were studied by EPR spectroscopy in the polycrystalline state in a range of 5–300 K. The forbidden transition line is observed in the EPR spectrum (Fig. 10) of complex **XVIII** at 5 K with a significant increase in the spectrometer sensitivity in the “halved” field. The spectrum is described by the orthorhombically distorted spin-Hamiltonian (2) of the dimer with the spin $S = 1$ and the Zeeman hyperfine and fine interactions

$$\begin{aligned} \hat{H} = & g_z\beta H_z S_z + g_x\beta H_x S_x + g_y\beta H_y S_y \\ & + AI_z S_z + BI_x S_x + CI_y S_y \\ & + D\left(S_z^2 - \frac{1}{3}S(S+1)\right) + E\left(S_x^2 - S_y^2\right). \end{aligned} \quad (2)$$

The following parameters were obtained by the simulation of the spectrum: $g_z = 2.196$, $g_x = 2.041$, $g_y = 2.009$, $A = 3.35 \times 10^{-3} \text{ cm}^{-1}$, $B = 2.59 \times 10^{-5} \text{ cm}^{-1}$, $C = 2.65 \times 10^{-3} \text{ cm}^{-1}$, $D = 2.77 \times 10^{-3} \text{ cm}^{-1}$, and $E = 2.20 \times 10^{-4} \text{ cm}^{-1}$.

In the case of complex **XIX**, the signal in the “halved” field is nearly absent even at 5 K. However, several features of the spectrum allowed the authors of the cited work to assume that the magnetic exchange interaction between the copper(II) ions also takes place in this case. The temperature evolution of the EPR spectra of complex **XIX** is shown in Fig. 11. It is noteworthy that the intensity of the spectrum at 20 K is higher than that at 5 K, whereas it is known from the EPR theory that the intensity of the EPR signal increases as the temperature decreases. The observed anomaly can be explained by intermolecular exchange interactions of the antiferromagnetic type with the isotropic exchange parameter $|J| \approx 1–5 \text{ cm}^{-1}$ in the sample of the complex [115].

The study of the temperature dependences of the magnetic susceptibility of complexes **XVIII** and **XIX** confirmed the existence of a very weak antiferromagnetic exchange interaction between the copper(II) ions. The effective magnetic moments of complexes **XVIII** and **XIX** based on one copper(II) ion are 1.88 and 1.91 μ_B at room temperature, whereas at 2 K $\mu_{\text{eff}} = 1.25$ and 1.35 μ_B , respectively. The exchange parameters for complex **XVIII** calculated by Eq. (1) are $2J = -3.0 \text{ cm}^{-1}$ and $zJ' = 0.55 \text{ cm}^{-1}$, and those for complex **XIX** are $2J = -2.6 \text{ cm}^{-1}$ and $zJ' = 0.60 \text{ cm}^{-1}$. These values are rather close to the value of $2J$ (-3.54 cm^{-1}) in the above described hydrogen-bound dimer of the **XVII** type in which the exchange interaction is also translated via the N—H···O hydrogen bonds and six atoms are localized between the interacting copper ions (chains of Cu—N—N···H—O—C—N—Cu bonds, copper—copper distance 4.431 Å).

The aforementioned role of noncovalent interactions in the formation of the magnetic properties of the supramolecular systems is illustrated by the results

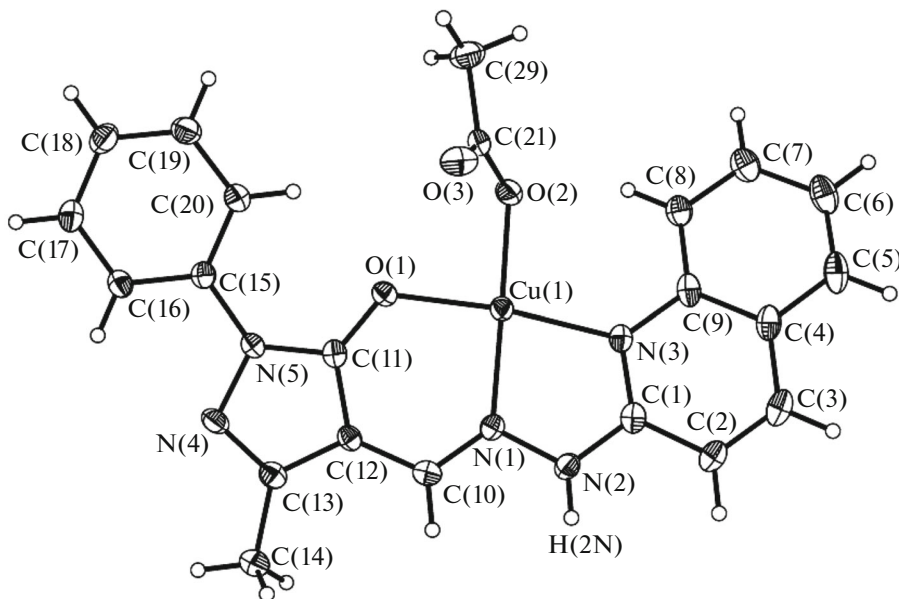


Fig. 4. Molecular structure of complex XVII [109].

[116] obtained for the synthesis and study of the spectral and magnetic properties of the polynuclear copper(II) complexes with isonicotinic acid, which is a convenient N,O-donor system and is suitable for the formation of supramolecular architectures of the complexes due to hydrogen bonds. Varying the synthesis conditions, the authors [116] succeeded to isolate two types of these structures (XX and XXI; Figs. 12, 13) differed in character of the ligand coordination and crystal chemical features of hydrogen bonding.

The study of the magnetic properties of the isolated supramolecular systems showed that compound XX represented, according to the definition of the authors [16], “quasi-2D magnet” with the exchange interaction between the paramagnetic centers over the hydrogen bond systems, whereas compound XXI is characterized by the intraferromagnetic exchange interaction of the ferromagnetic type along the Cu—O—Cu chain due to the shortening of the distance between the Cu²⁺ ions as asserted in [16]. The same research group [16] succeeded to preparatively isolate the supramolecular Cu²⁺ complexes with the *trans*-4,4'-azobis(pyridine) ligand system of two types [116]. The first type corresponds to the 1D coordination polymer with the anti-ferromagnetic exchange, whereas the complex of the second type forms the 2D polymer stabilized due to intermolecular hydrogen bonds for which the retention of the residual magnetization of the sample was experimentally proved.

The statement that relatively weak intermolecular interactions are a wonderful tool for the formation of supramolecular structures, including those with the controlled exchange interaction, was proved experimentally [117–121]. For example, the synthesis and

structures of seven supramolecular Mn(II), Co(II), Fe(II), Cu(II), Zn(II), and Cd(II) complexes based on tetrathiafulvalenetetracarboxylate (TC-TTF) and bipyridine (Bipy) of the general composition [M(Bipy)₂(H₂O)₄][M(TC-TTF)(H₂O)₂] were described [118]. The examples for the formation of cationic and anionic 1D chains in the case of Mn(II) ions (XXII), which are further self-organized into the 3D structure (Fig. 15) due to the O—H···O and O—H···N hydrogen bonds and π···π interaction, are presented in Fig. 14.

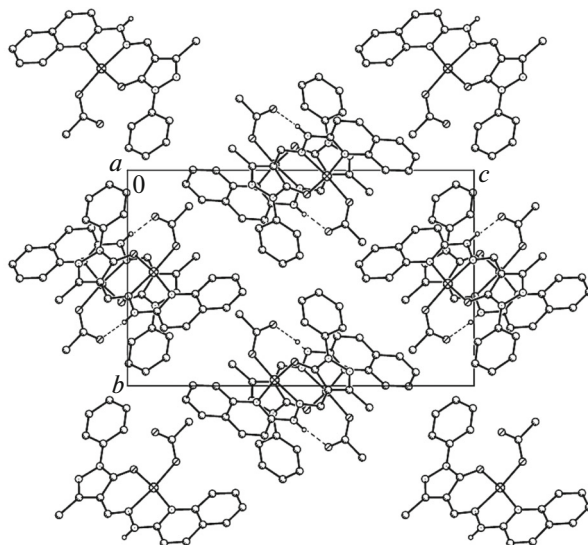


Fig. 5. Crystal packing of the dimers of complex XVII (view along the crystallographic axis *a*) [109].

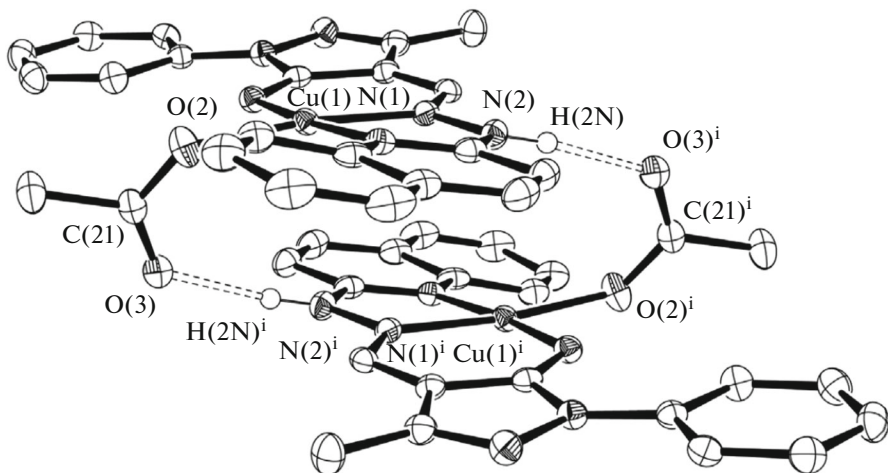


Fig. 6. Centrosymmetric dimers linked by the hydrogen bond [109].

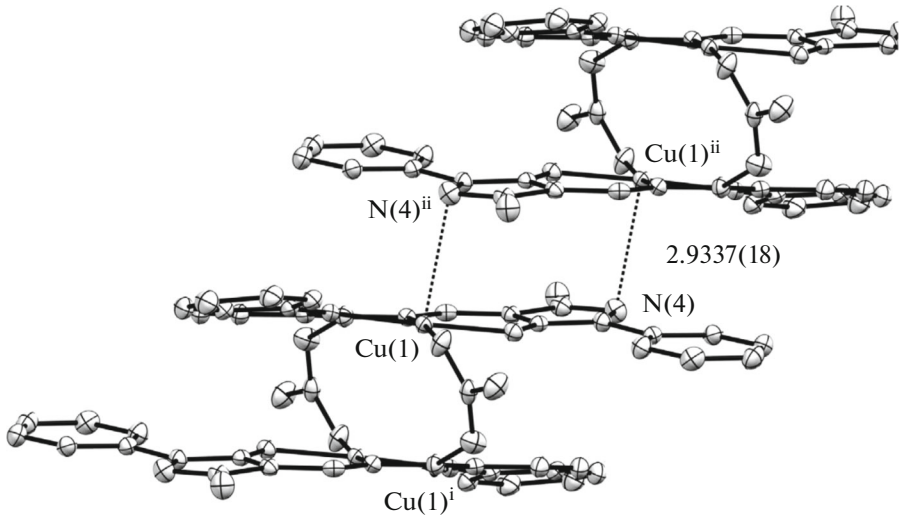


Fig. 7. Weak coordination between the hydrogen-bonded dimers [109].

Complex **XXII** has the properties of a trivial paramagnetic, but quite different situation was observed [122] for the tetranuclear and related supramolecular complexes. These complexes contain transition metal ions and also rare-earth ions, whose magnetochemical significance is caused by the pronounced magnetic anisotropy, which is one of the necessary conditions for the targeted design of SMM [123]. 4-Trifluoromethylbenzoic acid and 1,10-phenanthroline were chosen [122] as ligand systems owing to the known ability of carboxylate-containing ligands to act as both chelating agents and binding bridges. The structural fragments (a) and (b) (Fig. 16) are fairly easily joined into the 1D chain supramolecules (c) (**XXIII**) due to the hydrogen bonds.

An analysis of the dynamic magnetic susceptibility of complex **XXIII** unambiguously confirmed the slow

relaxation of the magnetization indicating in favor of the SMM character of the obtained compound.

III. TRANSITION METAL COMPLEXES CONTAINING THE CUBANE FRAGMENT WITH DIFFERENT EXCHANGE CHANNELS

For the recent decades, the polynuclear copper(II) complexes attract attention of researchers due to the formation of diverse coordination architectures and potential use in such areas as coordination polymers [124–126], magnetochemistry and bioinorganic chemistry [127–131], and catalysis [132–134]. Among them, the cubane-like Cu_4O_4 complexes containing hydroxo-, alkoxo-, or phenoxo-bridged fragments are worthy of special mentioning from the viewpoint of

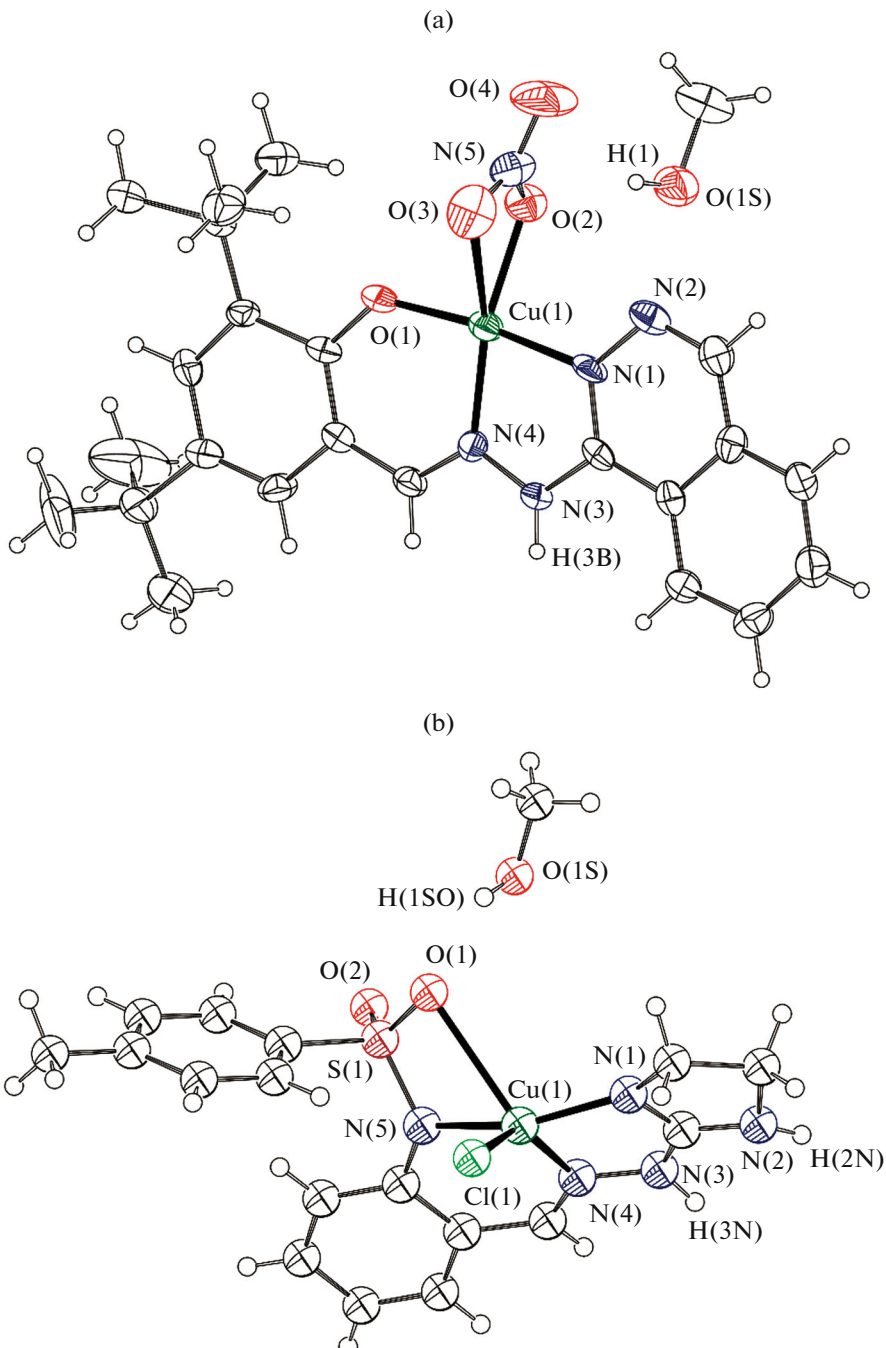


Fig. 8. Structures of complexes (a) XVIII and (b) XIX in the representation of atoms by thermal shift ellipsoids with 30% probability [114].

experimental and theoretical magnetochemistry [135–139].

Two structural classifications were proposed on the basis of structural features of the cubane-like Cu_4O_4 complexes. The chronologically first classification [140] was based on the Cu–O bond lengths in the cubane fragment. The approach to the second type of classification [141–143] was based on the Cu–Cu

bond lengths within the cubane moiety and made it possible to assign the complexes to three types (Fig. 17).

Although an analysis of the magnetic structural data for these complexes enabled one to reveal some parameters affecting the magnetic exchange in similar systems, no determining magnetic structural relationships were established. In addition, contradictory

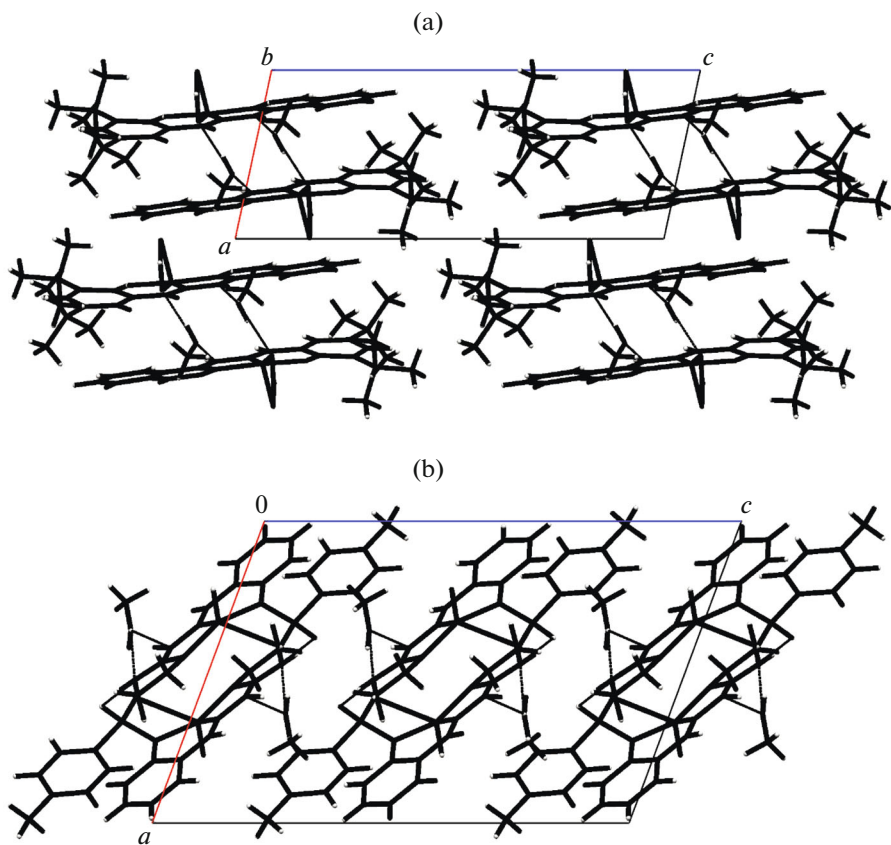


Fig. 9. Crystal packing of the hydrogen-bonded dimers of complexes (a) **XVIII** and (b) **XIX** (view along the crystallographic axis *b*) [114].

results were obtained for the complexes of the 4 + 2 type, the essence of which was the opposite signs of the exchange parameters obtained from the theoretical calculations and experimental data. As shown below, a

wide variety of the compositions and structures of the tetrานuclear complexes leads to a necessity of a detailed approach to the examination of the magnetic properties of these systems in order to obtain generalized magnetochemical regularities. A similar approach is exemplified by the data [144] on the synthesis of the supramolecular structures, which were analyzed in

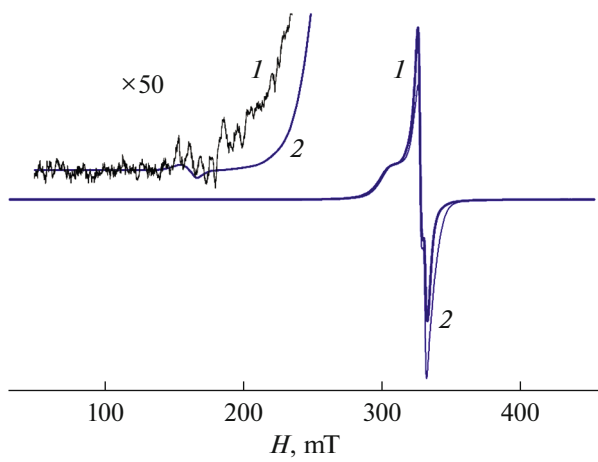


Fig. 10. EPR spectrum of the polycrystalline sample of complex **XVIII** at 5 K: (1) experiment and (2) theory. Inset (at upper left): the magnified region of the spectrum in the halved field [114].

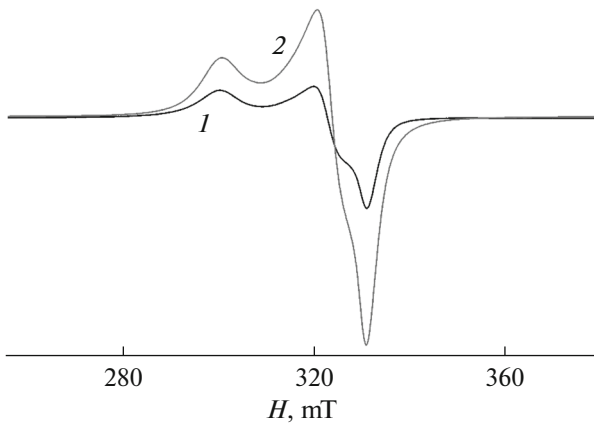


Fig. 11. Temperature evolution of the EPR spectra of complex **XIX**: 5 (1) and 20 K (2) [114].

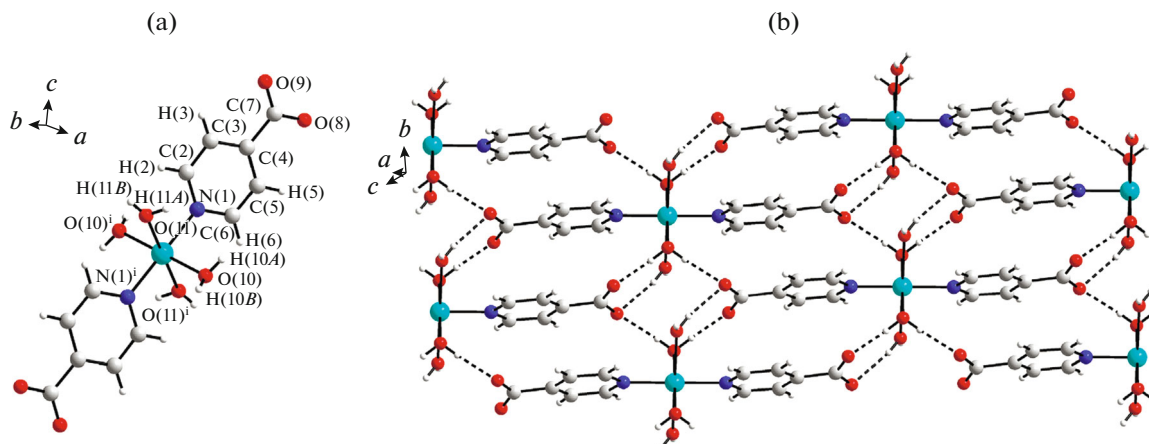


Fig. 12. (a) Fragment of the crystal structure of complex **XX** and (b) the 3D supramolecular structure of complex **XX** showing the formation of hydrogen bonds involving the water molecules and the uncoordinated carboxylate groups of the ligand molecule [116].

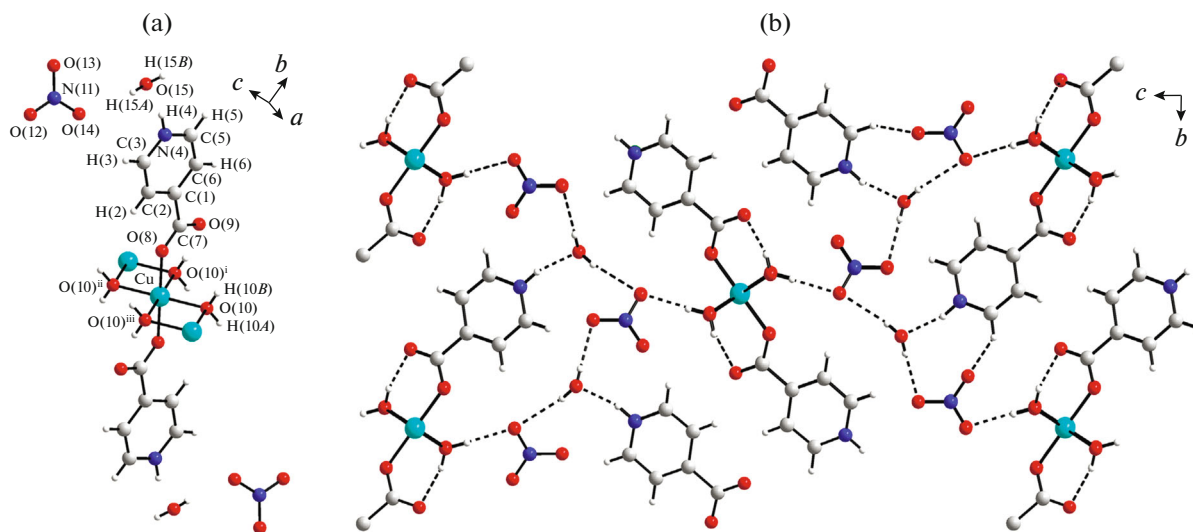


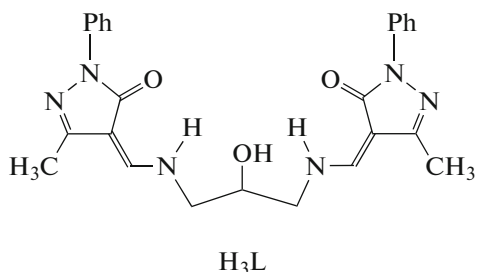
Fig. 13. (a) Fragment of the crystal structure of complex **XXI** and the hydrogen bonds between the individual fragments of **XXI** leading to the formation of (b) the 3D supramolecular architecture [116].

detail in the previous section. Metallocubanes $[\text{M}_4^{\text{II}}(\text{HL}^2)_4(\text{OAc})_4]$ of the **XXV** type, whose structure is shown in Fig. 18, were obtained by molecular self-assembling using 2,6-pyridinedimethanol (H_2L^2 , **XXIV**) and cobalt(II) and nickel(II) acetates.

The formation of the single crystals of **XXV** · $2\text{CH}_3\text{OH}$ is caused by the $\pi-\pi$ interaction and formation of both intra- and intermolecular $\text{O}-\text{H}\cdots\text{O}$ hydrogen bonds, resulting in the 3D architecture. The magnetic measurements proved the “mixed” character of the intramolecular exchange with the ferro- and antiferromagnetic parameters, the scheme of which is shown below as a figure in Table 3.

The crystal packing effects that affect the structural details and magnetic properties of the cubanes were

mentioned [145–149]. For example, the results of the XRD and magnetochemical studies are presented [149] for the tetranuclear copper(II) complex with the azomethine ligand, the product of condensation of 1-phenyl-3-methyl-4-formylpyrazolone-5 and 1,3-diaminopropanol-2 (H_3L).



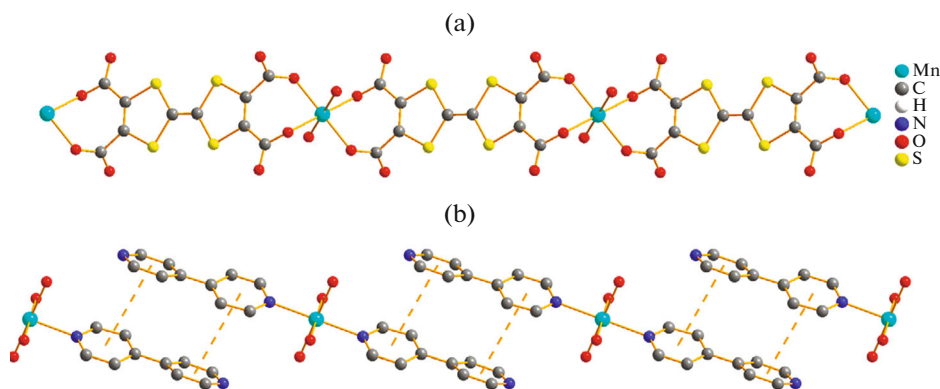


Fig. 14. (a) Anionic and (b) cationic 1D chains of complex XXII [118].

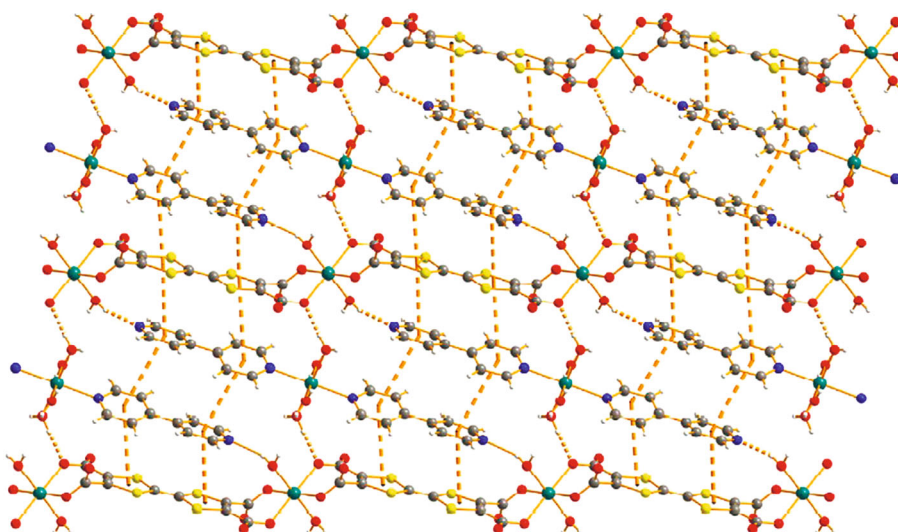


Fig. 15. Supramolecular 3D architecture of complex XXII [118].

The reaction of bis(azomethine) H_3L with copper(II) perchlorate in the presence of triethylamine and sodium azide followed by recrystallization from acetonitrile afforded complex **XXVI** of the composition $[\text{Cu}_{12}\text{L}_6(\text{N}_3)_6] \cdot 9\text{C}_2\text{H}_3\text{N} \cdot \text{H}_2\text{O}$. The symmetrically independent part of the unit cell of compound **XXVI** contains 1.5 molecules of the complex (**A** and **B**; **B** is localized in the partial position on the 2-fold symmetry axis), 4.5 acetonitrile molecules, and 0.5 water molecule. The ratio of molecules **A** and **B** in the unit cell is 2 : 1. The structures of both complexes **A** and **B** can formally be described as two binuclear fragments linked by the bridging azide groups (Fig. 19), which results in the formation of the distorted central cubic fragment $\text{Cu}_4\text{N}_2\text{O}_2$ in which the copper atoms occupy the vertices of the tetrahedron inscribed in this cube. The coordination modes of the copper atoms in the complexes differ, and the structures of these symmetrically independent molecules are also different. The most substantial distinction of

complexes **A** and **B** is manifested in the structures of their central cubic fragments $\text{Cu}_4\text{N}_2\text{O}_2$ (Fig. 20).

The shortest additional coordination in complex **A** is observed for the $\text{Cu}(3)$ atom ($\text{Cu}(3)-\text{O}(1) 2.289(3)$ Å) due to which the interpretation of the coordination polyhedron of the $\text{Cu}(3)$ atom as 4 + 1 (tetragonal pyramid) becomes doubtless. Molecule **B** has the symmetry C_2 , and the cubic fragment is distorted to a considerably lower extent. Both symmetrically independent copper atoms have the coordination mode 4 + 1. The distortions of the cubic fragment are also manifested in the $\text{Cu}\cdots\text{Cu}$ contacts. The distances between the copper atoms $\text{Cu}(2)\cdots\text{Cu}(3)$ and $\text{Cu}(3)\cdots\text{Cu}(4)$ in complex **A** are fairly short (2.9743(8) and 3.0187(9) Å, respectively), and the distance range is 2.97–4.03 Å. The range of $\text{Cu}\cdots\text{Cu}$ distances is somewhat shorter in the cubic fragment of molecule **B**: 3.17–3.92 Å. It seems most interesting that two conformations appreciably different in structures of both ligands and cubic fragments are observed in the same crystalline lattice

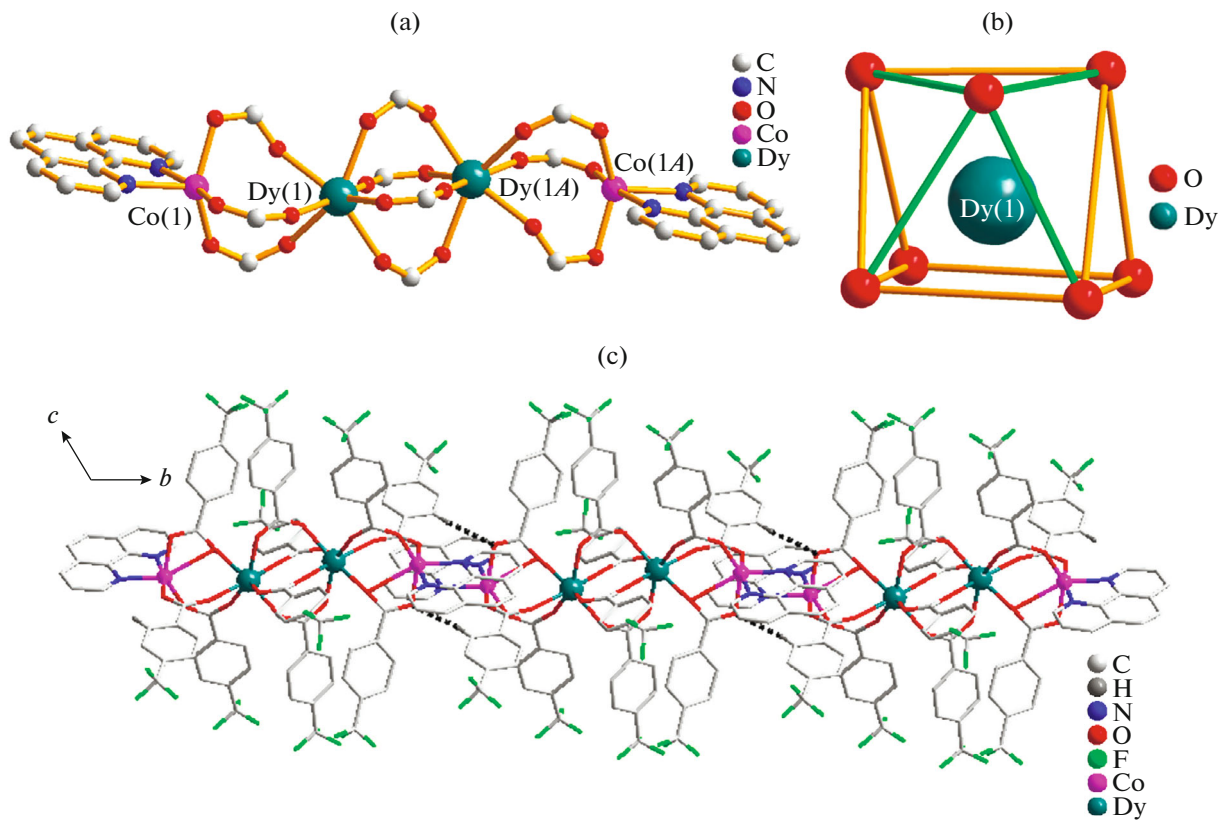


Fig. 16. (a, b) Structural fragments and (c) the supramolecular architecture of complex **XXIII** [122].

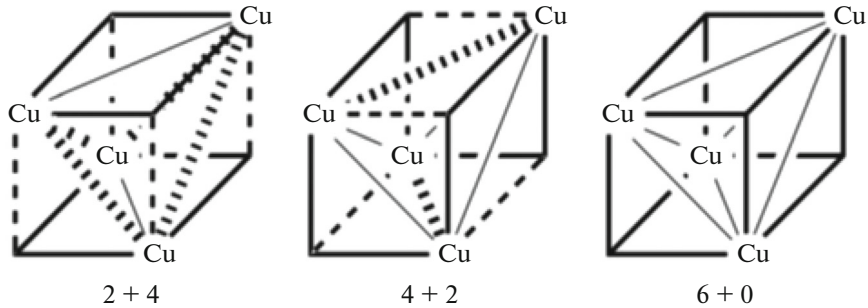


Fig. 17. Structural types of the complexes with the Cu₄O₄ cubane fragment classified according to the Cu...Cu distance (solid lines for short Cu...Cu and Cu–O distances, and dashed lines correspond to longer Cu...Cu and Cu–O bonds) [141].

of compound **XXVI**. A comparison of the structures of the complexes suggests that the copper atoms tend to form the stable coordination mode 4 + 1 characteristic of Cu(II) when the tetranuclear complex with the cubic geometry of the central Cu₄N₂O₂ fragment is formed. Evidently, the volume of the ligands affects the geometry of the cubic fragment. However, the manifestation of this influence shows that the symmetry of the cubic fragment can easily be distorted by an intermolecular interaction. The hydrogen bond between the water molecule and complex **A** observed

in the crystal structure is rather weak (O(1w)–H(1w)…N(14): H…N 2.240, O…N 3.028(5) Å, angle OHN 154°). The quantum chemical modeling allowed us to conclude that the presence of two conformers of the complex in the crystalline lattice is determined only by the intermolecular interaction in the solid state and packing effects rather than by specific features of the structures of the molecules, because the single conformation is theoretically most stable. The spin-Hamiltonian for cluster **A** is presented as Eq. (3)

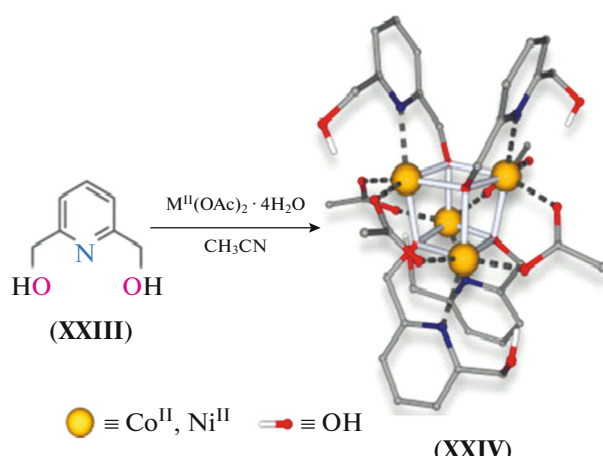


Fig. 18. Synthesis of cubanes $[\text{M}_4(\text{HL}^2)_4(\text{OAc})_4]$ ($\text{M} = \text{Co}^{2+}$ (**XXVa**), Ni^{2+} (**XXVb**)) [144].

$$\hat{H}_A = -J_1(\hat{S}_1\hat{S}_2 + \hat{S}_1\hat{S}_3) - J_2(\hat{S}_2\hat{S}_3) - J_3(\hat{S}_1\hat{S}_4 + \hat{S}_3\hat{S}_4), \quad (3)$$

and that for cluster **B** can be presented in the form of Eq. (4)

$$\hat{H}_B = -J_1(\hat{S}_1\hat{S}_2 + \hat{S}_1\hat{S}_2) - J_2(\hat{S}_1\hat{S}_1) - J_3(\hat{S}_1\hat{S}_2 + \hat{S}_1\hat{S}_2). \quad (4)$$

Accepting that the molar magnetic susceptibility of the complex is equal to the sum of susceptibilities of the “symmetric” and “nonsymmetric” clusters and assuming that the spin-Hamiltonian for both clusters includes three exchange parameters, we succeeded to satisfactorily describe the temperature dependence of the magnetic susceptibility of the complex at the following parameters of the model: $J_{1A} = -178$, $J_{2A} = 80$, $J_{3A} = 18$, $J_{1B} = -26$, $J_{2B} = -74$, and $J_{3B} = 46 \text{ cm}^{-1}$ and $g_A = g_B = 2.05$.

A combination of the ferro- and antiferromagnetic exchange channels is a rather general phenomenon for the exchange-bound cubane-like systems [150, 151], and the situations when the ferromagnetic contributions prevail are possible. For example, two copper(II) complexes of the compositions $\{[\text{Cu}(\text{H}_2\text{L}_1)]_4\}$ (**XXVII**) (H_2L_1 is *N*-(2-hydroxyethyl)-3,5-di-*tert*-butylsalicylaldimine) and $\{[\text{Cu}(\text{H}_2\text{L}_2)]_4$ (**XXVIII**) (H_2L_2 is *N*-(2-hydroxyethyl)-4-methoxysalicylaldimine) were synthesized [152]. Compounds **XXVII** and **XXVIII** were

shown [152] by XRD to be the tetranuclear alkoxo-bridged complexes containing substantially distorted cubane fragments Cu_4O_4 of the 4 + 2 type (Fig. 21).

The magnetic properties of both complexes correspond to the strong intramolecular exchange interaction of the ferromagnetic type leading to the ground state with the spin $S = 2$. Four short and two longer distances between the copper atoms (type 4 + 2) were detected in these compounds, which should imply, in our opinion, six different exchange channels and exchange parameters (Fig. 22).

In order to decrease the number of parameters, we assumed that the exchange interactions via the “short route” between the copper atoms are identical and described by the parameter J and the exchange channels corresponding to a longer interatomic distance are described by the parameter J' , which corresponds to the isotropic Hamiltonian (5)

$$H = -J(S_{\text{Cu}1}S_{\text{Cu}2} + S_{\text{Cu}1}S_{\text{Cu}3} + S_{\text{Cu}2}S_{\text{Cu}4} + S_{\text{Cu}3}S_{\text{Cu}4}) - J'(S_{\text{Cu}1}S_{\text{Cu}4} + S_{\text{Cu}2}S_{\text{Cu}3}). \quad (5)$$

The exchange parameters were $J = +28.7 \text{ cm}^{-1}$, $J' = +7.8 \text{ cm}^{-1}$, and $g = 2.036$ for complex **XXVII** and $J = +39.8 \text{ cm}^{-1}$, $J' = +10.2 \text{ cm}^{-1}$, and $g = 2.025$ for complex **XXVIII**.

The DFT calculations give good correspondence of the theoretical and experimental values of exchange parameters by both the sign and value, and the complexes of the **XXVII** and **XXVIII** types represent one of rare examples of cubane-like structures in which the exchange interaction between the copper atoms is exclusively ferromagnetic.

As mentioned above for tetranuclear complex **XXVI**, the exchange channel involving the azide bridge with the coordination mode of the μ -1,1 character corresponds to the ferromagnetic interaction. A similar situation takes place for the tetranuclear coordination compound $[\text{Mn}_4(\text{L})_2(\text{CH}_3\text{OH})_2(\mu\text{-N}_3)_4(\text{N}_3)_2] \cdot 2(\text{CH}_3\text{OH})$ (**XXIX**) described earlier [153], whose structure is presented in Fig. 23a, where L is the deprotonated form of bis[(*E*)-*N*-(phenyl(pyridin-2-yl)methylene)]carbohydrazide.

The tetranuclear fragment in complex **XXIX** contains two exchange effects of the bridge differed in the character of translation: the ferromagnetic azide effect and the antiferromagnetic enolate effect prevailing in the absolute value of the exchange parameter. This provides the general antiferromagnetic character of

Table 3. Exchange parameters and factors for cubanes **XXVa** and **XXVb**

Compound	J_1	J_1 [K]	J_2 [K]	G
XXVa		10.8	-14.7	2.0
XXVb		52.3	-4.2	2.2

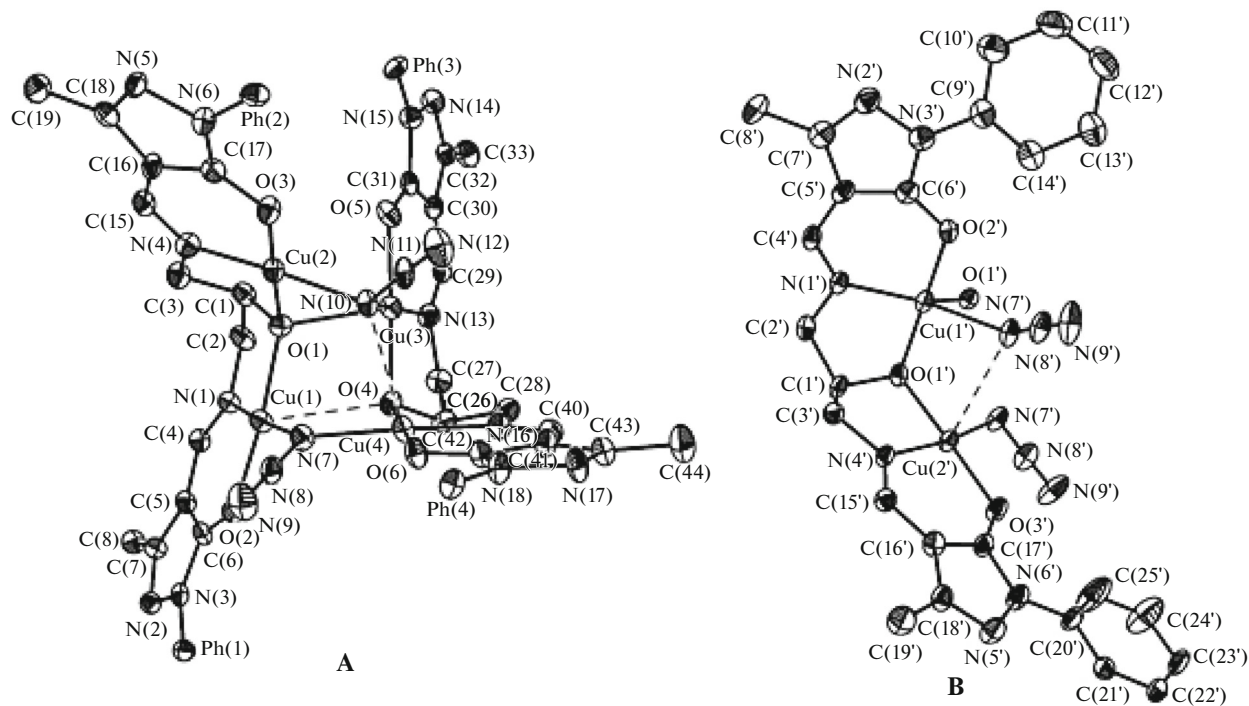


Fig. 19. General view of molecules **A** and **B** of complex **XXVI** in the representation of atoms by atomic shift ellipsoids with 50% probability (hydrogen atoms are omitted, phenyl groups of molecule **A** are replaced by designation Ph, and only the symmetry-independent part is shown for molecule **B** except for the coordination modes of the Cu atoms shown completely) [149].

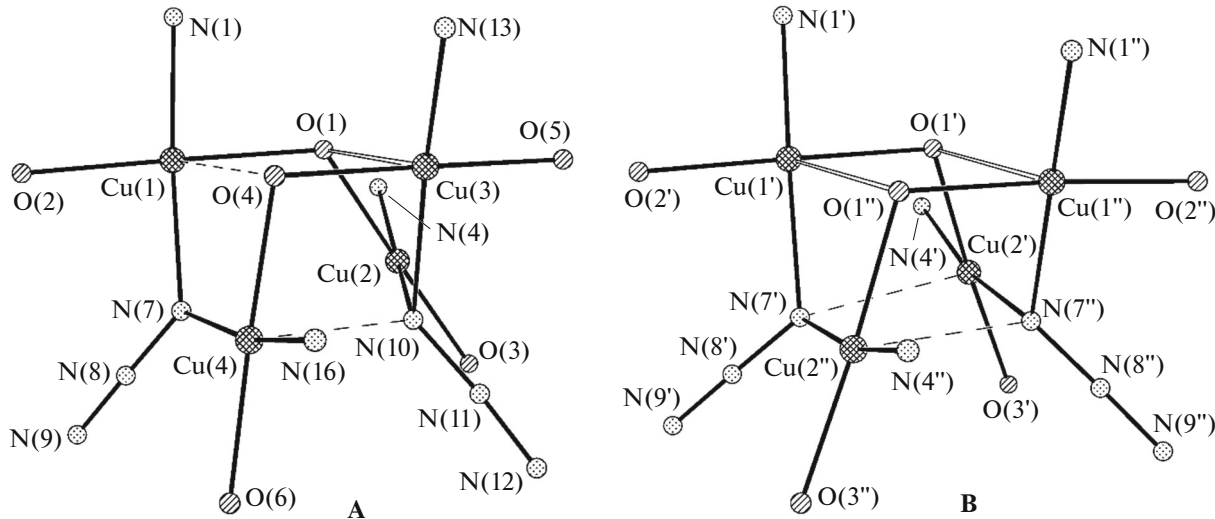


Fig. 20. Structures of the exchange fragments in molecules **A** and **B** of complex **XXVI** (only the donor atoms of the ligands and the N_3^- bridging groups are shown) [149].

exchange. The spin-Hamiltonian of the system takes the following form:

$$H = -2J_1(\hat{S}_1\hat{S}_2 + \hat{S}_3\hat{S}_4) - 2J_2(\hat{S}_1\hat{S}_4 + \hat{S}_2\hat{S}_3) \quad (6)$$

with the parameters $g = 1.98$, $J_1 = +1.1 \text{ cm}^{-1}$, and $J_2 = -1.3 \text{ cm}^{-1}$.

The theoretical calculations also predict the ferromagnetic character of exchange via the channel $\text{Mn}-(\mu-1,1-\text{N}_3)_2-\text{Mn}$ if the bond angle α_N of the $\text{Mn}-\text{N}-\text{Mn}$ fragment is $\sim 100^\circ$. According to this statement, the exchange parameter $J_1 = +1.1 \text{ cm}^{-1}$ undoubtedly corresponds to the channel with the $(\mu-1,1-\text{N}_3)_2$ bridging fragment ($\alpha_{\text{average}} = 100.85^\circ$) in complex

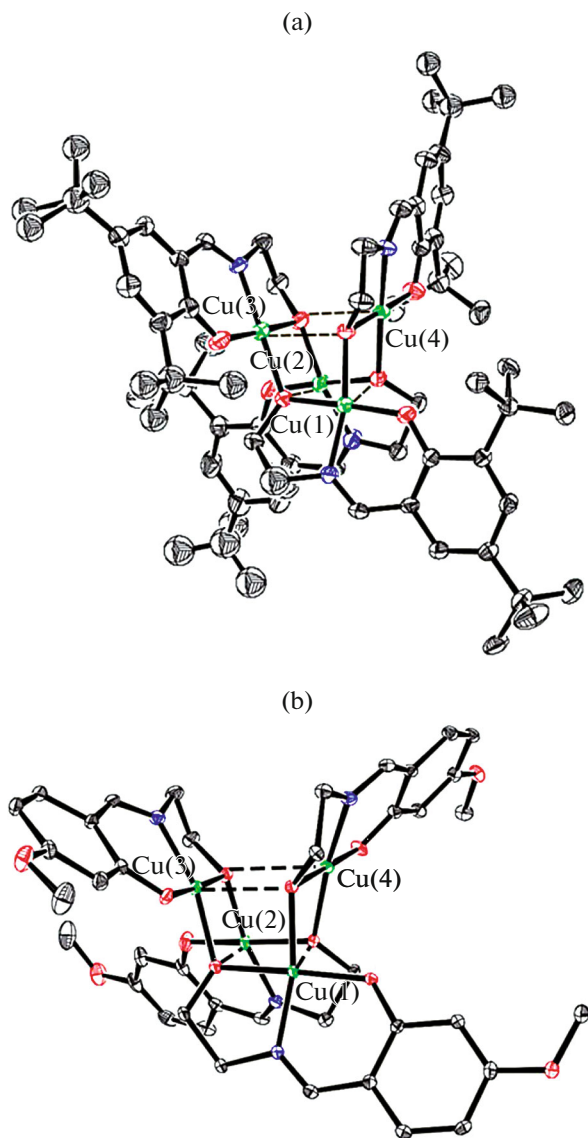


Fig. 21. Structures of complexes (a) **XXVII** and (b) **XXVIII** (hydrogen atoms are omitted) [152].

XXIX, and the parameter $J_2 = -1.3 \text{ cm}^{-1}$ describes the exchange interaction via the enolic oxygen atom.

A similar dependence of the exchange parameters on the MXM bond angle in the exchange fragment was also observed in the work [154] devoted to the physicochemical study of the nickel(II) complex of the **XXX** type with the composition $[\text{Ni}_4(\mu_3\text{-OH})_4(\mu\text{-L}_m)_2(\text{DMF})_4]\text{ClO}_4 \cdot \text{DMF} \cdot \text{EtOH}$, where L_m is *m*-bis[bis(1-pyrazolyl)methyl]benzene, whose structure is shown in Fig. 23b.

As mentioned earlier [154], if the Ni_4 core has the tetrahedral symmetry, six exchange parameters J_{ij} should be equal. However, the detailed analysis of the XRD data revealed two fragments with different NiONi bond angles: the bond angle in the first frag-

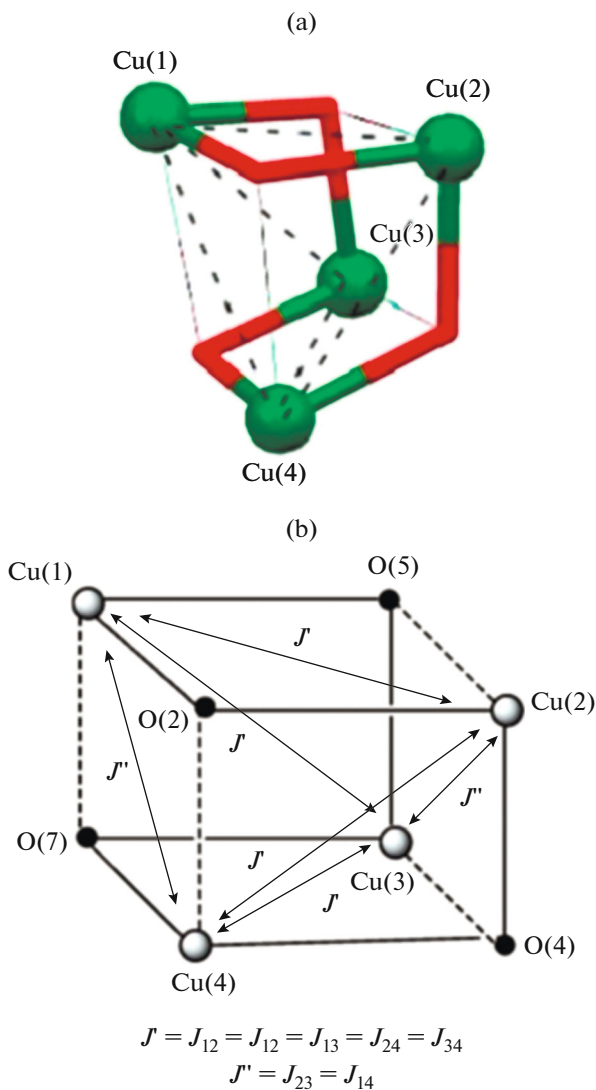


Fig. 22. (a) Structures of the exchange fragments in the molecules of complexes **XXVII**–**XXVIII** and (b) potential exchange channels [152].

ment lies in a range of 97.9° – 99.5° , and the angle range in the second fragment is 100.3° – 101.5° . Therefore, two ferromagnetic exchange channels can be expected in this case, and the first channel will be predominant. In this case, the exchange Hamiltonian takes the form

$$\hat{H}_{\text{HDVV}} = -J_1(\hat{S}_1\hat{S}_2 + \hat{S}_2\hat{S}_4 + \hat{S}_3\hat{S}_4) - J_2(\hat{S}_1\hat{S}_3 + \hat{S}_1\hat{S}_4 + \hat{S}_2\hat{S}_3) \quad (7)$$

with the parameters $J_1 = 9.1 \text{ cm}^{-1}$ and $J_2 = 2.1 \text{ cm}^{-1}$. The obtained results are confirmed by the DFT calculations.

To conclude, in this review we attempted to present the possibilities of the magnetochemical method used for the description of the structures and properties of the bi- and tetranuclear metallochelates and supramo-

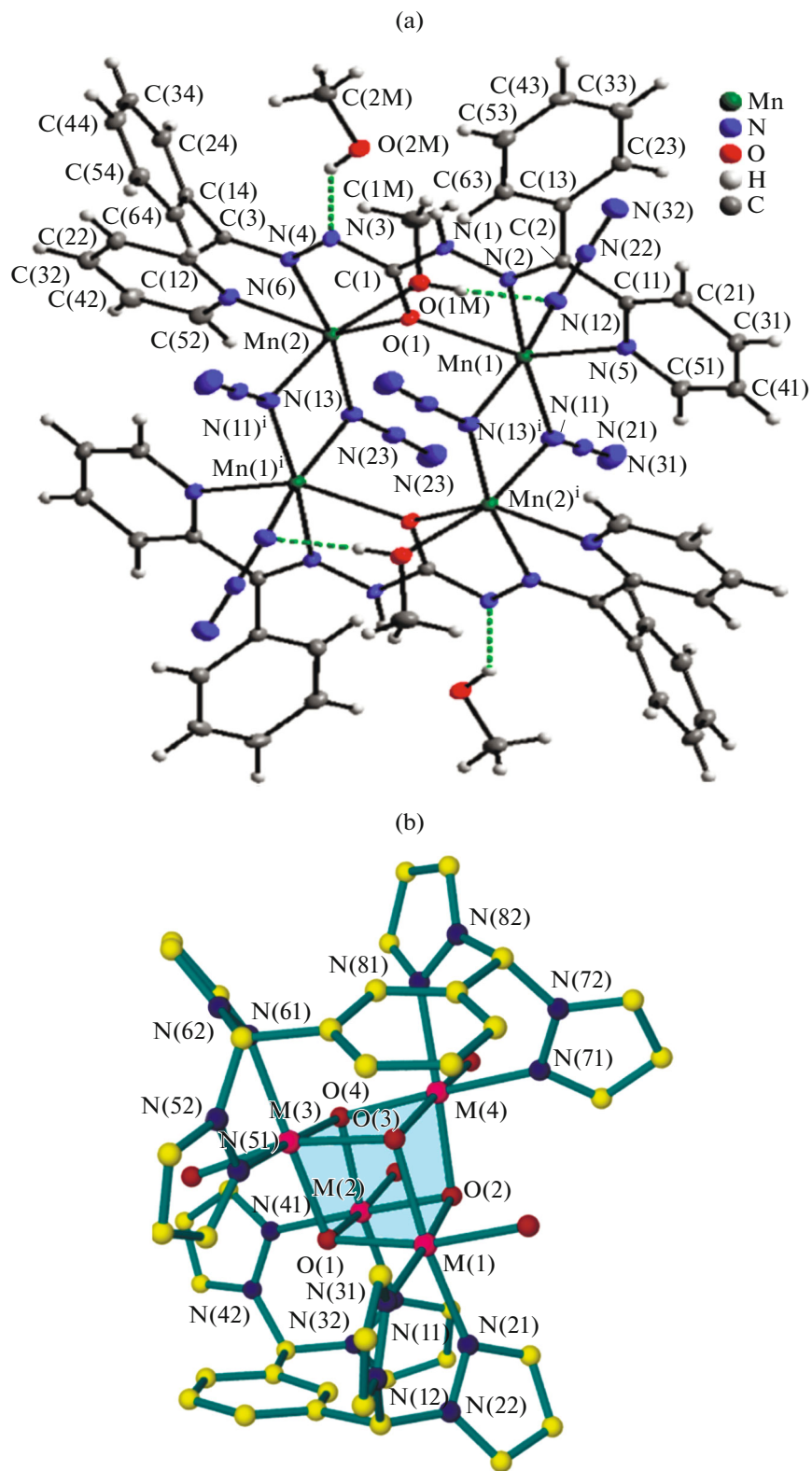


Fig. 23. Structures of complexes (a) XXIX [153] and (b) XXX [154].

lecular architectures based on coordination compounds with restricted types of ligand systems, mainly hydrazones, azomethines, and their analogs. We tried to elucidate the range of most important problems that were solved using the magnetochemical method predominantly for the exchange-ligand systems with the indicated ligands. Obviously, the further theoretical and experimental development of the magnetochemical method in respect of the adequate interpretation of the properties of similar systems is a very urgent task, especially for the targeted design of supramolecular structures with specified or controlled physicochemical characteristics and for revealing the fundamental regularities of the structure–property relationship aimed at preparing new materials, for example, molecular magnetics for innovative technologies of the nearest future. Significant possibilities of coordination chemistry in respect of producing multifunctional single-molecule magnets with unique magnetic, electronic, optical, redox, and photochemical properties provide an important potential for the scientific society. It is doubtless that the systematization of the presently available vast material on these problems, which was started in the reviews and monographs cited above, will be continued in generalized studies of research groups working in various areas of the modern coordination chemistry.

ACKNOWLEDGMENTS

This work was carried out in the framework of the development program of the Southern Federal University (internal grant no. VnGr-07/2017-29).

REFERENCES

1. Itoh, K. and Kinoshita, M., *Molecular Magnetism: New Magnetic Materials*, Tokio: Kodansha and Gordon & Breach Science, 2000.
2. *Magnetism: Molecules to Materials: Models and Experiments*, Miller J.S. and Drillon, M., Eds., Weimheim: Wiley-VCH, 2001.
3. Launay, J.P. and Verdaguer, M., *Electrons in Molecules: From Basic Principles to Molecular Electronics*, Oxford: Oxford University, 2014.
4. Joachim, C., Gimzewski, J.K., and Aviram, A., *Nature*, 2000, vol. 408, p. 541.
5. Park, J., Pasupathy, A.N., Goldsmith, J.I., et al., *Nature*, 2002, vol. 417, p. 722.
6. Smith, R.H.M., Noat, Y., Untiedt, C., et al., *Nature*, 2002, vol. 419, p. 906.
7. Ng, M.K., Lee, D.C., and Yu, L., *J. Am. Chem. Soc.*, 2002, vol. 124, p. 11862.
8. Carroll, R.L. and Gorman, C.B., *Angew. Chem., Int. Ed. Engl.*, 2002, vol. 41, p. 4378.
9. Lippard, S.J. and Berg, J.M., *Principles of Bioinorganic Chemistry*, California: Univ. Sci. Books, Mill Valley, 1994.
10. Que, L., Jr. and Dong, Y., *Acc. Chem. Res.*, 1996, vol. 29, p. 190.
11. Law, N.A., Caudle, M.T., and Pecoraro, V.L., *Adv. Inorg. Chem.*, 1998, vol. 46, p. 305.
12. Wu, A.J., Penner-Hahn, J.E., and Pecoraro, V.L., *Chem. Rev.*, 2004, vol. 104, p. 903.
13. Herrero, C., Lassalle-Kaiser, B., Leibl, W., et al., *Coord. Chem. Rev.*, 2008, no. 252, p. 456.
14. Kärkäs, M.D., Verho, O., Johnston, E.V., et al., *Chem. Rev.*, 2014, vol. 114, p. 11863.
15. Gerey, B., Gouré, E., Fortage, J., et al., *Coord. Chem. Rev.*, 2016, no. 319, p. 1.
16. Engelmann, X., Monte-Pérez, I., and Ray, K., *Angew. Chem., Int. Ed. Engl.*, 2016, vol. 55, p. 7632.
17. Ferrando-Soria, J., Vallejo, J., Castellano, M., et al., *Coord. Chem. Rev.*, 2017, vol. 339, p. 17.
18. Clemente-León, M., Coronado, E., Martí-Gastaldo, C., et al., *Chem. Soc. Rev.*, 2011, vol. 40, p. 473.
19. Muñoz, M.C. and Real, J.A., *Coord. Chem. Rev.*, 2011, vol. 255, p. 2068.
20. Guo, J.F., Yeng, W.F., and Gao, S., *Eur. J. Inorg. Chem.*, 2008, p. 158.
21. Coronado, E. and Mínguez-Espallargas, G., *Chem. Soc. Rev.*, 2013, vol. 42, p. 1525.
22. Grancha, T., Ferrando-Soria, J., Castellano, M., et al., *Chem. Commun.*, 2014, vol. 50, p. 7569.
23. Ouahab, L., *Multifunctional Molecular Materials*, Singapore: Pan Standford, 2013.
24. Ferrando-Soria, J., Ruiz-García, R., Cano, J., et al., *Chem.-Eur. J.*, 2012, vol. 18, p. 1608.
25. Sessoli, R., Boulon, M.-E., Caneschi, A., et al., *Nat. Phys.*, 2015, vol. 10, no. 1, p. 69.
26. Chorazy, S., Nakabayashi, K., Ohkoshi, S., et al., *Chem. Mater.*, 2014, vol. 26, p. 4072.
27. Pardo, E., Train, C., Gontard, G., et al., *J. Am. Chem. Soc.*, 2011, vol. 133, p. 15328.
28. Risset, O.N., Quintero, P.A., Brinzari, T.V., et al., *J. Am. Chem. Soc.*, 2014, vol. 136, p. 15660.
29. Darago, L.E., Aubrey, M.L., Yu, C.J., et al., *J. Am. Chem. Soc.*, 2015, vol. 137, p. 15703.
30. Jeon, I.-R., Sun, L., Negru, B., et al., *J. Am. Chem. Soc.*, 2016, vol. 138, p. 6583.
31. Pinkowicz, D., Rams, M., Misek, M., et al., *J. Am. Chem. Soc.*, 2015, vol. 137, p. 8795.
32. Romero-Morcillo, T., Dela Pinta, D., Callejo, L.M., et al., *Chem.-Eur. J.*, 2015, no. 21, p. 12112.
33. Trzop, E., Zhang, D., Pineiro-Lopez, L., et al., *Angew. Chem., Int. Ed. Engl.*, 2016, vol. 55, p. 8675.
34. Clements, J.E., Price, J.R., Neville, S.M., et al., *Angew. Chem., Int. Ed. Engl.*, 2016, vol. 55, p. 15105.
35. Reed, D.A., Xiao, D.J., Gonzalez, M.I., et al., *J. Am. Chem. Soc.*, 2016, vol. 138, p. 5594.
36. Hay, J.P., Thibeault, J.C., and Hoffmann, R., *J. Am. Chem. Soc.*, 1975, vol. 97, p. 4884.
37. Kahn, O. and Briat, B., *J. Chem. Soc., Faraday Trans. 2*, 1976, vol. 268, p. 79.
38. Girerd, J.J., Joumaux, Y., and Kahn, O., *Chem. Phys. Lett.*, 1981, vol. 82, p. 534.
39. Kahn, O., Galy, J., Joumaux, Y., et al., *J. Am. Chem. Soc.*, 1982, vol. 104, p. 2165.

40. Julve, M., Verdaguer, M., Gleizes, A., et al., *Inorg. Chem.*, 1984, vol. 23, p. 3808.

41. Julve, M., Faus, J., Verdaguer, M., et al., *J. Am. Chem. Soc.*, 1984, vol. 106, p. 8306.

42. Willet, R., Gatteschi, D., and Kahn, O., *Magneto-Structural Correlations in Exchange-Coupled Systems (NATO ASI Series C)*, Dordrecht: D. Reidel., 1985.

43. Kahn, O., *Angew. Chem., Int. Ed. Engl.*, 1985, vol. 24, p. 834.

44. Kahn, O., *Z. Anorg. Allg. Chem.*, 1987, vol. 68, p. 89.

45. Blondin, G. and Girerd, J.J., *Chem. Rev.*, 1990, vol. 90, p. 1359.

46. Kogan, V.A., Lukov, V.V., and Shcherbakov, I.N., *Russ. J. Coord. Chem.*, 2010, vol. 36, no. 6, p. 401. doi 10.1134/S1070328410060011

47. Lukov, V.V., Shcherbakov, I.N., Levchenkov, S.I., et al., *Russ. J. Coord. Chem.*, 2017, vol. 43, no. 1, p. 1. doi 10.1134/S1070328417010055

48. Kalinnikov, V.T. and Rakitin, Yu.V. *Vvedenie v magnetokhimiyu. Metod staticheskoi magnitnoi vospriimchivosti* (Introduction to Magnetochemistry. Static Magnetic Susceptibility Method), Moscow: Nauka, 1980.

49. Rakitin, Yu.V. and Kalinnikov, V.T. *Sovremennaya magnetokhimiya* (Modern Magnetochemistry), St. Petersburg: Nauka, 1994.

50. Kalinnikov, V.T., Rakitin, Yu.V., and Novotortsev, V.M., *Russ. Chem. Rev.*, 2003, vol. 72, no. 12, p. 995.

51. Shchegolkov, E.V., Burgart, Ya.V., Khudina, O.G., et al., *Russ. Chem. Rev.*, 2010, vol. 79, no. 1, p. 31.

52. Hakki, E., Safak, C., Mevlut, E., et al., *J. Indian. Chem. Soc.*, 1989, vol. 66, p. 45.

53. Mishra, P., Gupta, P.N., and Shakya, A.K., *J. Indian. Chem. Soc.*, 1991, vol. 68, p. 618.

54. Likhate, M.A. and Fernandes, P.S., *J. Indian. Chem. Soc.*, 1990, vol. 67, p. 862.

55. Badr, M.Z.A., Mahmoud, M.A., Mahgoub, S.A., et al., *Bull. Pol. Acad. Sci. Chem.*, 1989, vol. 37, p. 185.

56. Revankar, V.K., Arali, V.H., and Mehale, V.B., *Indian. J. Chem. A*, 1990, vol. 29, p. 889.

57. Bartolucci, C., Cellai, L., Patrizia, F., et al., *Farmaco*, 1992, vol. 41, p. 945.

58. Vicini, P., Incerti, M., Doychinova, I.A., et al., *Eur. J. Med. Chem.*, 2006, vol. 41, p. 624.

59. Odashima, T., Yamaguchi, M., and Ishii, H., *Microchim. Acta*, 1991, vol. 1, p. 267.

60. Sakamoto, H., Ishikawa, J., Nakagamo, H., et al., *Chem. Lett.*, 1992, vol. 21, p. 481.

61. Levchenkov, S.I., Popov, L.D., Shcherbakov, I.N., et al., *Russ. J. Gen. Chem.*, 2014, vol. 84, no. 10, p. 1970.

62. Abramenco, V.L., Garnovskii, A.D., Abramenco, Yu.V., *Koord. Khim.*, 1994, vol. 20, no. 1, p. 39.

63. Lukov, V.V., Kogan, V.A., Bogatyreva, E.V., et al., *Zh. Neorg. Khim.*, 1989, vol. 34, no. 10, p. 2554.

64. Bogatyreva, E.V., Kogan, V.A., Lukov, V.V., et al., *Zh. Neorg. Khim.*, 1990, vol. 35, no. 8, p. 2010.

65. Kogan, V.A. and Lukov, V.V., *Koord. Khim.*, 1993, vol. 19, no. 6, p. 476.

66. Lukov, V.V., Tupolova, Yu.P., Kogan, V.A., et al., *Russ. J. Coord. Chem.*, 2003, vol. 29, no. 5, p. 335.

67. Levchenkov, S.I., Kogan, V.A., and Lukov V.V., *Zh. Neorg. Khim.*, 1993, vol. 38, no. 12, p. 1992.

68. Lukov, V.V., Levchenkov, S.I., and Kogan, V.A., *Zh. Neorg. Khim.*, 1997, vol. 42, no. 4, p. 606.

69. Lukov, V.V., Levchenkov, S.I., and Kogan V.A., *Koord. Khim.*, 1998, vol. 24, no. 12, p. 946.

70. Kogan, V.A., Lukov, V.V., Levchenkov, S.I., et al., *Mendeleev Commun.*, 1998, no. 4, p. 145.

71. Iskander, M.F., El-Sayed, L., Salem, N.M.H., et al., *Polyhedron*, 2004, vol. 23, no. 1, p. 23.

72. Starikov, A.G., Kogan, V.A., Lukov, V.V., et al., *Russ. J. Coord. Chem.*, 2009, vol. 35, no. 8, p. 616. doi 10.1134/S1070328409080090

73. Tandon, S.S., Thompson, L.K., and Hynes, R.C., *Inorg. Chem.*, 1992, vol. 31, p. 2210.

74. Brooker, S., Davidson, T.C., Hay, S.J., et al., *Coord. Chem. Rev.*, 2001, vol. 216, p. 3.

75. Popov, L.D., Levchenkov, S.I., Shcherbakov, I.N., et al., *Russ. J. Gen. Chem.*, 2010, vol. 80, no. 3, p. 493.

76. Sangeetha, N.R., Baradi, R., Gupta, R., et al., *Polyhedron*, 1999, vol. 18, p. 1425.

77. Haba, P.M., Diouf, O., Sy, A., et al., *Z. Kristallogr. Cryst. Mater.*, 2005, vol. 220, p. 479.

78. Chan, S.C., Koh, L.L., Leung, P.-H., et al., *Inorg. Chim. Acta*, 1995, vol. 236, p. 101.

79. Roth, A., Buchholz, A., Gärtner, V., et al., *Z. Anorg. Allgem. Chem.*, 2007, vol. 633, p. 2009.

80. Simonov, Yu.A., Bourosh, P.N., Yampol'skaya, M.A., et al., *Koord. Khim.*, 1990, vol. 16, no. 8, p. 1072.

81. Yamamoto, T., *X-ray Spectrom.*, 2008, vol. 37, p. 572.

82. Kochubei, D.I., Babanov, Yu.A., Zamaraev, K.I., et al., *Rentgenospektral'nyi metod izucheniya struktury amorfnykh tel: EXAFS-spektroskopiya* (X-ray Spectroscopic Method for Studying the Structure of Amorphous Solids: EXAFS Spectroscopy) Novosibirsk: Nauka. Sib. Otd-nie, 1988.

83. Popov, L.D., Levchenkov, S.I., Shcherbakov, I.N., et al., *Russ. J. Coord. Chem.*, 2011, vol. 37, no. 7, p. 483. doi 10.1134/S1070328411060078

84. Geary, W.J., *Coord. Chem. Rev.*, 1971, vol. 7, no. 1, p. 81.

85. Kogan, V.A., Levchenkov, S.I., Popov, L.D., et al., *Ros. Khim. Zh.*, 2009, vol. 53, no. 1, p. 86.

86. Tandon, S.S., Thompson, L.K., and Hynes, R.C., *Inorg. Chem.*, 1992, vol. 31, p. 2210.

87. Abraham, F., Lagrenée, M., Sueur, S., et al., *J. Chem. Soc., Dalton Trans.*, 1991, p. 1443.

88. Popov, L.D., Levchenkov, S.I., Shcherbakov, I.N., et al., *Russ. J. Gen. Chem.*, 2010, vol. 80, no. 12, p. 2501.

89. Popov, L.D., Mishchenko, A.V., Tupolova, Yu.P., et al., *Russ. J. Gen. Chem.*, 2011, vol. 81, no. 8, p. 1691.

90. Popov, L.D., Levchenkov, S.I., Shcherbakov, I.N., et al., *Russ. J. Gen. Chem.*, 2012, vol. 82, no. 3, p. 465.

91. Popov, L.D., Shcherbakov, I.N., Levchenkov, S.I., et al., *J. Coord. Chem.*, 2008, vol. 61, no. 3, p. 392.

92. Popov, L.D., Tupolova, Yu.P., Lukov, V.V., et al., *Inorg. Chim. Acta*, 2009, vol. 362, no. 6, p. 1673.

93. Tupolova, Yu.P., Popov, L.D., Lukov, V.V., et al., *Z. Anorg. Allg. Chem.*, 2009, vol. 635, no. 3, p. 530.

94. Bryleva, M.A., Kravtsova, A.N., Shcherbakov, I.N., et al., *Russ. J. Struct. Chem.*, 2012, vol. 53, no. 2, p. 295.

95. Castro, I., Calatayud, M.L., Barros, W.P., et al., *Inorg. Chem.*, 2014, vol. 53, p. 5759.

96. Shcherbakov, I.N., Levchenkov, S.I., Popov, L.D., et al., *Russ. J. Coord. Chem.*, 2015, vol. 41, no. 2, p. 69. doi 10.1134/S1070328415020098

97. Pavlishchuk, A.V., Satska, Yu.A., Kolotilov, S.V., et al., *Cur. Inorg. Chem.*, 2015, vol. 5, p. 5.

98. Hazra, S., Karmakar, A., Silva, M., et al., *Inorg. Chem. Commun.*, 2014, vol. 46, p. 113.

99. Liu, X., Cen, P., Li, H., et al., *Inorg. Chem.*, 2014, vol. 53, p. 8088.

100. Ogawa, H., Mori, K., Murashima, K., et al., *Inorg. Chem.*, 2016, vol. 55, p. 717.

101. Atzori, M., Serpe, A., Deplano, P., et al., *Inorg. Chem. Front.*, 2015, vol. 2, p. 108.

102. Biswas, R., Mukherjee, S., Ghosh, S., et al., *Inorg. Chem. Commun.*, 2015, vol. 56, p. 108.

103. Desplanches, C., Ruiz, E., Rodríguez-Forstea, A., et al., *J. Am. Chem. Soc.*, 2002, vol. 124, p. 5197.

104. Desplanches, C., Ruiz, E., and Alvarez, S., *Chem. Commun.*, 2002, p. 2614.

105. Bandeira, N.A.G. and Guennic, B.L., *J. Phys. Chem. A*, 2012, vol. 116, p. 3465.

106. Bandeira, N.A.G., Maynau, D., Robert, V., et al., *Inorg. Chem.*, 2013, vol. 52, p. 7980.

107. Perić, M., Zlatar, M., Grubišić, S., et al., *Polyhedron*, 2012, vol. 42, p. 89.

108. Rakitin, Yu.V., Kalinnikov, V.T., Khodasevich, S.G., and Novotortsev, V.M., *Russ. J. Coord. Chem.*, 2007, vol. 33, no. 8, p. 551. doi 10.1134/S1070328407080015

109. Levchenkov, S.I., Shcherbakov, I.N., Popov, L.D., et al., *Inorg. Chim. Acta*, 2013, vol. 405, p. 169.

110. Larin, G.M., Shul'gin, V.F., Mel'nikova, E.D., Zub, V.Y., and Rakitin, Yu.V., *Russ. Chem. Bull., Int. Ed.*, 2002, vol. 51, no. 4, p. 632.

111. Popov, L.D., Levchenkov, S.I., Shcherbakov, I.N., et al., *Russ. J. Coord. Chem.*, 2013, vol. 39, no. 12, p. 849. doi 10.1134/S1070328413110079

112. Popov, L.D., Levchenkov, S.I., Shcherbakov, I.N., et al., *Russ. J. Struct. Chem.*, 2015, vol. 56, no. 1, p. 102.

113. Levchenkov, S.I., Shcherbakov, I.N., Popov, L.D., et al., *Russ. J. Gen. Chem.*, 2013, vol. 83, no. 10, p. 1928.

114. Levchenkov, S.I., Popov, L.D., Efimov, N.N., et al., *Russ. J. Inorg. Chem.*, 2015, vol. 60, no. 9, p. 1129. doi 10.1134/S0036023615040129

115. Larin, G.M., Minin, V.V., and Shul'gin, V.F., *Russ. Chem. Rev.* 2008, vol. 77, no. 5, p. 451.

116. Almáši, M., Vargová, Z., Gyepes, R., et al., *Inorg. Chem. Commun.*, 2014, vol. 46, p. 118.

117. Qian, J., Hu, J., Yoshikawa, H., et al., *Eur. J. Inorg. Chem.*, 2015, p. 2110.

118. Qin, J.-H., Chang, X.-H., Ma, L.-F., et al., *Inorg. Chem. Commun.*, 2015, vol. 41, p. 92.

119. Song, J.H., Lim, K.S., Ryu, D.W., et al., *Inorg. Chem.*, 2014, vol. 53, p. 7936.

120. Tan, X., Ji, X., and Zheng, J.-M., *Inorg. Chem. Commun.*, 2015, vol. 60, p. 27.

121. Sessoli, R. and Powell, A., *Coord. Chem. Rev.*, 2009, vol. 253, p. 2328.

122. Tan, X., Ji, X., and Zheng, J.-M., *Inorg. Chem. Commun.*, 2015, vol. 60, p. 27.

123. Sessoli, R. and Powell, A., *Coord. Chem. Rev.*, 2009, vol. 253, p. 232.

124. Adams, C.J., Kurawa, M.A., Lusi, M., et al., *CrystEngComm*, 2008, vol. 10, p. 1790.

125. Chang, M., Chung, M., Lee, B.S., et al., *Nanosci. Nanotechnol.*, 2006, vol. 6, p. 3338.

126. Kang, S.G., Kim, H., and Bang, S., *Inorg. Chim. Acta*, 2013, vol. 396, p. 10.

127. Coronado, E. and Day, P., *Chem. Rev.*, 2004, vol. 104, p. 5419.

128. Liu, C.M., Xiong, R.G., Zhang, D.Q., et al., *J. Am. Chem. Soc.*, 2010, vol. 132, p. 4044.

129. Lu, Z., Fan, T., Guo, W., et al., *Inorg. Chim. Acta*, 2013, vol. 400, p. 191.

130. Henkel, G. and Krebs, B., *Chem. Rev.*, 2004, vol. 104, p. 801.

131. Tjioe, L., Meininge, A., Joshi, T., et al., *Inorg. Chem.*, 2011, vol. 50, p. 4327.

132. Wegner, R., Gottschaldt, M., Görls, H., et al., *Chem.-Eur. J.*, 2001, vol. 7, p. 2143.

133. Diaz-Requejo, M.M. and Pérez, P.J., *Chem. Rev.*, 2008, vol. 108, p. 3379.

134. Safaei, E., Kabir, M.M., Wojtczak, A., et al., *Inorg. Chim. Acta*, 2011, vol. 366, p. 275.

135. Lu, J.W., Huang, Y.H., Lo, S., et al., *Inorg. Chem. Commun.*, 2007, vol. 10, p. 1210.

136. Monfared, H.H., Sanchiz, J., Kalantari, Z., et al., *Inorg. Chim. Acta*, 2009, vol. 362, p. 3791.

137. Ruiz, E., Alvarez, S., Rodríguez-Forstea, A., et al., *J. Mater. Chem.*, 2006, vol. 16, p. 2729.

138. Ruiz, E., Alvarez, S., Rodríguez-Forstea, A., et al., *Electronic Structure and Magnetic Behavior in Polynuclear Transition-Metal Compounds*, Weinheim: Wiley-VCH, 2001, vol. 1.

139. Ruiz, E., Rodríguez-Forstea, A., Alemany, P., et al., *Polyhedron*, 2001, vol. 20, p. 1323.

140. Mergehenn, R. and Haase, W., *Acta Crystallogr., Sect. B: Struct. Crystallogr. Cryst. Chem.*, 1977, vol. 33, p. 1877.

141. Tercero, J., Ruiz, E., Alvarez, S., Rodríguez-Forstea, A., and Alemany, P., *J. Mater. Chem.*, 2006, vol. 16, p. 2729.

142. Ruiz, E., Alvarez, S., Rodríguez-Forstea, A., et al., *Electronic Structure and Magnetic Behavior in Polynuclear Transition-Metal Compounds*, Weinheim: Wiley-VCH, 2001, vol. 2, p. 227.

143. Ruiz, E., Rodríguez-Forstea, A., Alemany, P., et al., *Polyhedron*, 2001, vol. 20, p. 1323.

144. Scheurer, A., Korzekwa, J., Nakajima, T., et al., *Eur. J. Inorg. Chem.*, 2015, vol. 2015, p. 1892.

145. Carter, K.P., Thomas, K.E., Pope, S.J.A., et al., *Inorg. Chem.*, 2016, vol. 55, p. 6902.

146. Costes, J.-P., Duhayon, C., and Vendier, L., *Inorg. Chem.*, 2014, vol. 53, p. 2181.

147. Li, Y., Guo, Y., Tian, H., et al., *Inorg. Chem. Commun.*, 2014, vol. 43, p. 135.

148. Tian, C.-B., He, C., Han, Y.-H., et al., *Inorg. Chem.*, 2015, vol. 54, p. 2560.

149. Levchenkov, S.I., Shcherbakov, I.N., Popov, L.D., et al., *Russ. J. Coord. Chem.*, 2014, vol. 40, no. 2, p. 69. doi 10.1134/S1070328414020055

150. Gao, Y.-Z., Zhang, Y.-A., and Zhang, J., *Inorg. Chem. Commun.*, 2015, vol. 54, p. 85.

151. Dias, S.S.P. and Kirillova, M.V., André, V., et al., *Inorg. Chem.*, 2015, vol. 54, p. 5204.

152. Gungor, E., Kara, H., Colacio, E., et al., *Eur. J. Inorg. Chem.*, 2014, p. 1552.

153. Bikas, R., Hosseini-Monfared, H., Siczek, M., et al., *Inorg. Chem. Commun.*, 2015, vol. 62, p. 60.

154. Reger, D.L., Pascui, A.E., Pellechia, P.J., et al., *Inorg. Chem.*, 2014, vol. 53, no. 9, p. 4325.

Translated by E. Yablonskaya